NASA/TM—2001-210753

Thermodynamic Database for the $NdO_{1.5}$-$YO_{1.5}$-$YbO_{1.5}$-$ScO_{1.5}$-ZrO_2 System

Nathan S. Jacobson and Evan H. Copland
Glenn Research Center, Cleveland, Ohio

Larry Kaufman
Consultant, Brookline, Massachusetts

September 2001

The NASA STI Program Office . . . in Profile

Since its founding, NASA has been dedicated to the advancement of aeronautics and space science. The NASA Scientific and Technical Information (STI) Program Office plays a key part in helping NASA maintain this important role.

The NASA STI Program Office is operated by Langley Research Center, the Lead Center for NASA's scientific and technical information. The NASA STI Program Office provides access to the NASA STI Database, the largest collection of aeronautical and space science STI in the world. The Program Office is also NASA's institutional mechanism for disseminating the results of its research and development activities. These results are published by NASA in the NASA STI Report Series, which includes the following report types:

- TECHNICAL PUBLICATION. Reports of completed research or a major significant phase of research that present the results of NASA programs and include extensive data or theoretical analysis. Includes compilations of significant scientific and technical data and information deemed to be of continuing reference value. NASA's counterpart of peer-reviewed formal professional papers but has less stringent limitations on manuscript length and extent of graphic presentations.
- TECHNICAL MEMORANDUM. Scientific and technical findings that are preliminary or of specialized interest, e.g., quick release reports, working papers, and bibliographies that contain minimal annotation. Does not contain extensive analysis.
- CONTRACTOR REPORT. Scientific and technical findings by NASA-sponsored contractors and grantees.
- CONFERENCE PUBLICATION. Collected papers from scientific and technical conferences, symposia, seminars, or other meetings sponsored or cosponsored by NASA.
- SPECIAL PUBLICATION. Scientific, technical, or historical information from NASA programs, projects, and missions, often concerned with subjects having substantial public interest.
- TECHNICAL TRANSLATION. English-language translations of foreign scientific and technical material pertinent to NASA's mission.

Specialized services that complement the STI Program Office's diverse offerings include creating custom thesauri, building customized data bases, organizing and publishing research results . . . even providing videos.

For more information about the NASA STI Program Office, see the following:

- Access the NASA STI Program Home Page at ***http://www.sti.nasa.gov***
- E-mail your question via the Internet to help@sti.nasa.gov
- Fax your question to the NASA Access Help Desk at 301–621–0134
- Telephone the NASA Access Help Desk at 301–621–0390
- Write to:
  NASA Access Help Desk
  NASA Center for AeroSpace Information
  7121 Standard Drive
  Hanover, MD 21076

NASA/TM—2001-210753

Thermodynamic Database for the $NdO_{1.5}$-$YO_{1.5}$-$YbO_{1.5}$-$ScO_{1.5}$-ZrO_2 System

Nathan S. Jacobson and Evan H. Copland
Glenn Research Center, Cleveland, Ohio

Larry Kaufman
Consultant, Brookline, Massachusetts

National Aeronautics and
Space Administration

Glenn Research Center

September 2001

Available from

NASA Center for Aerospace Information
7121 Standard Drive
Hanover, MD 21076

National Technical Information Service
5285 Port Royal Road
Springfield, VA 22100

Available electronically at http://gltrs.grc.nasa.gov/GLTRS

THERMODYNAMIC DATABASE FOR THE $NdO_{1.5}$-$YO_{1.5}$-$YbO_{1.5}$-$ScO_{1.5}$-ZrO_2 SYSTEM

Nathan S. Jacobson and Evan H. Copland
National Aeronautics and Space Administration
Glenn Research Center
Cleveland, Ohio 44135

Larry Kaufman
Consultant
Brookline, Massachusetts 02445

SUMMARY

A database for $YO_{1.5}$-$NdO_{1.5}$-$YbO_{1.5}$-$ScO_{1.5}$-ZrO_2 for ThermoCalc* has been developed. The basis of this work is the $YO_{1.5}$-ZrO_2 assessment by Du et al. (ref. 1). Experimentally only the $YO_{1.5}$-ZrO_2 system has been well-studied. All other systems are only approximately known. The major simplification in this work is the treatment of each single cation unit as a component. The pure liquid oxides are taken as reference states and two term lattice stability descriptions are used for each of the components. The limited experimental phase diagrams are reproduced.

I. INTRODUCTION

The rare earth oxide stabilized zirconias are of considerable technological importance. Applications range from thermal barrier coatings for turbine blades to electrodes for sensors and fuel cells. The most widely used system is Y_2O_3-ZrO_2. The phase diagram for this system has been extensively studied (refs. 2 to 11) Further, there are several thermodynamic assessments and calculated phase diagrams in the literature for this and related systems (refs. 1, 12 to 19).

In this report we also consider the stabilizers: Yb_2O_3, Sc_2O_3, and Nd_2O_3. These different stabilizers alone and in combinations may offer improved properties. However, both experimental phase diagrams and thermodynamic data for these systems are very limited (refs. 20 to 30). Reliable phase and thermodynamic information over a range of compositions and temperatures is essential to understand the processing and properties of zirconia with Y_2O_3, Yb_2O_3, Sc_2O_3, and Nd_2O_3 stabilizers.

Figures 1 to 10 give the available psuedo-binary phase diagrams for the systems (refs. 22 to 30) listed in table I. The most complete and most recent phase diagrams are given. In the case of Y_2O_3-ZrO_2, two phase diagrams are shown in figures 1(a) and (b). The first diagram from Stubican et al. (refs. 11 and 22) includes one intermediate compound—$Zr_3Y_4O_{12}$. The second diagram (ref. 23) also includes an ordered hexagonal phase—ZrY_6O_{12}. However, the existence of the second compound remains controversial and will not be considered here. In addition, the primary interest is in the ZrO_2-rich portion of the diagram and therefore its existence is not important in the present study. Figures 2(a) and (b) are the available diagrams for the Yb_2O_3-ZrO_2 system. Figure 2(a) primarily shows the liquidus and figure 2(b) shows the solid phases. Note that these are similar to the Y_2O_3-ZrO_2 diagram and shows an analogous intermediate phase—$Zr_3Yb_4O_{12}$. However $Zr_3Yb_4O_{12}$ is stable to 1612 °C and $Zr_3Y_4O_{12}$ is stable to only to 1250 °C (fig. 1(a)) or 1330 °C (fig. 1(b)). Figures 3 to 10 are the remaining available binaries. Most of these diagrams are incomplete and have many approximate boundaries.

The addition of two (or more) stabilizing rare earth oxides to zirconia may lead to some interesting properties. Yet only a portion of the Y_2O_3-Yb_2O_3-ZrO_2 ternary diagram has been determined experimentally (ref. 31). Three isothermal sections are shown in figures 11(a) to (c). The major features of these systems are a continuous solid solution of tetragonal zirconia and cubic zirconia with both Y_2O_3 and Yb_2O_3. Note also that the two intermediate compounds—$Zr_3Y_4O_{12}$ and $Zr_3Yb_4O_{12}$ connect at lower temperatures. At higher temperatures $Zr_3Y_4O_{12}$ becomes unstable and only $Zr_3Yb_4O_{12}$ protrudes into the ternary. At the highest temperatures, both compounds are unstable. No other ZrO_2 rare earth oxide experimental ternaries were found.

The first calculations of these types of refractory oxide phase diagrams were done in 1988 by Kaufman (ref. 14). Kaufman treats each oxide unit as a component. He sets the liquid oxide as a reference state and uses two-term lattice stabilities to describe each end point oxide. Thus the lattice stability of a particular polymorph becomes

*ThermoCalc AB, Stockholm, Sweden.

the energy to form that polymorph from the liquid. Du et al., (refs. 1 and 15) have done two assessments of the Y_2O_3-ZrO_2, using the Lukas programs (ref. 32) to derive phase descriptions that best fit all the available experimental data. Their first assessment (ref. 1) also uses the liquid as the reference state. Their second assessment (ref. 15) invokes the standard element reference state (SER) and uses Gibbs energy expressions for each phase.

This report discusses the development of a Thermo-Calc database for the multicomponent system: Nd_2O_3-Sc_2O_3-Yb_2O_3-Y_2O_3-ZrO_2. The quantities of Du et al., for ZrO_2-Y_2O_3 (ref. 1) are used directly and other binaries are developed based on this. Du et al., (ref. 1) perform two optimizations for the ZrO_2-Y_2O_3 system—using a different set of liquidus data for each optimization. Their second optimization values are used here. The rare earth oxides are normalized to one cation: $NdO_{1.5}$-$ScO_{1.5}$-$YbO_{1.5}$-$YO_{1.5}$-ZrO_2. Each of these one cation oxide units are treated as a component. Two-term lattice stability phase descriptions referenced to the liquid state are used, which are less complex than the Gibbs energy phase descriptions based on the standard element reference state.

The entire database in standard Thermo-Calc *.tdb format is given in appendix I. In the following report, we discuss this database and the calculation of binary and higher order diagrams in the Nd_2O_3-Sc_2O_3-Yb_2O_3-Y_2O_3-ZrO_2 system.

II. LATTICE STABILITIES FOR END-POINTS

In order to estimate the lattice stabilities with respect to the liquid state, we need the enthalpies and entropies for the polymorphic transformations. Only limited information is available, particularly on the solid/solid transformations. These data (refs. 33 to 35) are shown in table II. As noted, each oxide is normalized to one mole of cation. The oxide abbreviations are given in table III.

It is important to discuss the compositional difference between the calculations and the measured values in table II and figures 1 to 11. The experimental phase diagrams are for RE_2O_3-ZrO_2 (RE = Rare Earth Element) and will be referred to as such; the calculated diagrams are for $REO_{1.5}$-ZrO_2 and will be referred to as such. In order to compare the two, we need to convert from mole fraction $x(RE_2O_3)$, in RE_2O_3-ZrO_2 to mole fraction $x(REO_{1.5})$, in $REO_{1.5}$-ZrO_2. Note that

$$x(RE_2O_3 \text{ in } RE_2O_3-ZrO_2)=\frac{n(RE_2O_3 \text{ in } RE_2O_3-ZrO_2)}{n(RE_2O_3 \text{ in } RE_2O_3-ZrO_2)+n(ZrO_2 \text{ in } RE_2O_3-ZrO_2)} \quad (1)$$

Here n is the number of moles. The composition for $REO_{1.5}$-ZrO_2 is:

$$x(REO_{1.5} \text{ in } REO_{1.5}-ZrO_2)=\frac{n(REO_{1.5} \text{ in } REO_{1.5}-ZrO_2)}{n(REO_{1.5} \text{ in } REO_{1.5}-ZrO_2)+n(ZrO_2 \text{ in } REO_{1.5}-ZrO_2)} \quad (2)$$

Note that for each composition $n(ZrO_2)$ the same and that $n(RE_2O_3) = ½\, n(REO_{1.5})$. So now:

$$x(REO_{1.5})=\frac{2x(RE_2O_3)}{2x(RE_2O_3)+(1-x(RE_2O_3))} \quad (3)$$

Table IV shows the equivalent compositions.

Now consider the derivation of the lattice stabilities for each oxide. The most information is available for ZrO_2, which undergoes three transformations (ref. 36):

$$ZrO_2\text{: Monoclinic} \rightarrow \text{Tetragonal} \rightarrow \text{Cubic} \rightarrow \text{Liquid} \quad (4)$$

The approach of Kaufman (ref. 14) and ThermoCalc notation are used in the following discussion.

The liquid phase is taken as the reference state and thus:

$$G(L, ZM; 0) = 0.0 \quad (5)$$

For the cubic phase:

$$G(C,ZM;0) = \Delta H^{C\text{-}L} - T\,\Delta S^{C\text{-}L} = -87027 + 29.471T \tag{6}$$

This is the value from Kubachewski and Alcock (ref. 33) with a melting point of 2953 K. More recent investigations have given the melting point of cubic zirconia as 2983 K. Du and Jin (ref. 1) adjust equation (6) to reflect this:

$$G(C, ZM; 0) = -87986.6 + 29.496T \tag{7}$$

The tetragonal to cubic transformation temperature is given as 2568 K (33) and thus:

$$\Delta H^{T\text{-}C} - T\,\Delta S^{T\text{-}C} = -5941 + 2.313T \tag{8}$$

Again Du and Jin (ref. 1) adjust this for a more recent transformation temperature of 2642 K:

$$\Delta H^{T\text{-}C} - T\,\Delta S^{T\text{-}C} = -5941 + 2.249T \tag{9}$$

In order to obtain the free energy of the tetragonal phase referenced to the liquid, equations (7) and (9) are added:

$$G(T, ZM; 0) = \Delta H^{T\text{-}L} - T\,\Delta S^{T\text{-}L} = -93927 + 31.745T \tag{10}$$

From equation (10) a 'melting point' for the tetragonal phase can be calculated to be 2959 K. A metastable melting point must always be less than the melting point of the stable phase.

Table II indicates some disagreement on the monoclinic to tetragonal transformation temperature and heat. Here we take the temperature as 1454 K and the heat as 6000 joules/mol:

$$\Delta H^{M\text{-}T} - T\,\Delta S^{M\text{-}T} = -6000 + 4.127T \tag{11}$$

The free energy of the monoclinic phase referenced to the liquid is obtained by adding equations (10) and (11):

$$G(M, ZM; 0) = \Delta H^{M\text{-}L} - T\,\Delta S^{M\text{-}L} = -99927 + 35.872T \tag{12}$$

For the other oxides—$YO_{1.5}$, $YbO_{1.5}$, $NdO_{1.5}$, $ScO_{1.5}$–a similar approach was followed. However, less data is available. Of these the most data is available for $YO_{1.5}$. $YO_{1.5}$ undergoes two phase transformations:

$$YO_{1.5}\text{: Cubic} \rightarrow \text{Hexagonal} \rightarrow \text{Liquid} \tag{13}$$

Again, the liquid phase is taken as the reference state:

$$G(L, YM; 0) = 0.0 \tag{14}$$

The melting point of the hexagonal phase is accepted as 2712 K. Kaufman (ref. 14) estimates the lattice stability of the hexagonal phase as:

$$G(H,YM; 0) = \Delta H^{H\text{-}L} - T\,\Delta S^{H\text{-}L} = -56735 + 20.92T \tag{15}$$

This enthaply is somewhat more than half the IVTAN (ref. 34) data for melting of Y_2O_3, but more in line with Kubachewski's (ref. 34) values for alumina heat of melting (54 kJ/mol $AlO_{1.5}$).

The only measured transition heat for the polymorphs of a rare earth oxide was that for Y_2O_3 cubic to hexagonal, as reported in IVTAN to be 54 kJ/mol. However, this number seems much too high for a solid/solid transition such as this. Kaufman (ref. 14) estimates the heat to be about 10 kJ/mol and it seems more reasonable to use this value. Accepting the cubic to hexagonal transformation temperature of 2550 K the lattice stability for the cubic phase becomes:

$$G(C,YM; 0) = \Delta H^{C\text{-}L} - T\,\Delta S^{C\text{-}L} = -67419 + 25.105T \tag{16}$$

The behavior of $YbO_{1.5}$ is controversial. The two published phase diagrams with $YbO_{1.5}$ do not agree. The $YbO_{1.5}$-ZrO_2 diagram (fig. 2) indicates that the hexagonal phase melts; whereas the $YbO_{1.5}$-$NdO_{1.5}$ diagram (fig. 9) indicates that the cubic phase melts. It is assumed that the hexagonal phase of $YbO_{1.5}$ melts, in analogy with $YO_{1.5}$. Therefore the phase sequence with temperature is taken as:

$YbO_{1.5}$: Cubic → Hexagonal → Liquid

For $NdO_{1.5}$, the phase sequence with temperature appears to be:

$NdO_{1.5}$: N phase → Hexagonal → Cubic → Liquid

Little information is available for $ScO_{1.5}$ and it is assumed that the cubic phase melts. From the melting points and estimated heats of fusion, the lattice stabilities are derived as shown in the database (appendix I)

III. INTERACTION PARAMETERS: CUBIC, MONOCLINIC, TETRAGONAL, N PHASE, NM PHASE

In the binary case, each of the above solution phases are described by the following expression for the free energy:

$$G_m(x,T) = \sum_{i=1}^{2} x_i\,{}^{o}G_i(T) + RT\sum_{i=1}^{2} x_i \ln x_i + {}^{ex}G_m \tag{17}$$

The first term is the sum of the lattice stabilities for each of two components. These are discussed in the previous section. The Calphad approach requires a lattice stability for every component in each phase—even if a particular component does not form the phase described. For example, a lattice stability if necessary for hexagonal ZrO_2, monoclinic $YO_{1.5}$, and tetragonal $YO_{1.5}$. The lattice stabilities are chosen so that these phases are always unstable (Appendix I).

The second term in equation (17) is the random mixing term for an ideal solution. The third term is the excess Gibbs energy and accounts for the deviations from ideality. Many solution models have been developed for this term (refs. 37 to 39). In the Calphad approach, the excess Gibbs energy is expanded as a Redlich-Kister polynomial (ref. 37):

$${}^{ex}G_m = x_1 x_2 \sum_{j=0}^{n} {}^{j}L (x_1 - x_2)^j \tag{18}$$

Here only the first two terms are considered:

$${}^{ex}G_m = x_1 x_2\,{}^{o}L + x_1 x_2\,{}^{1}L(x_1 - x_2) = x_1 x_2\,{}^{o}L + x_1 x_2\,{}^{1}L(1 - 2x_2) \tag{19}$$

where ${}^{o}L$ and ${}^{1}L$ are the zero and first order interaction parameters, respectively. In assigning mole fraction designations, ThermoCalc takes the components in alphabetical order. Thus in this case $x_2 = x_{ZrO_2}$ and the sign of the second term in equation (19) is always the opposite of the sign of ${}^{1}L$ for $x_2 > 0.5$.

The shape of the Gibbs energy curves versus composition and temperature determine the stable phase fields in a classical temperature-composition phase diagram. The first two terms in equation (17) are fixed and lead to an ideal solution, as discussed in many textbooks (refs. 38 to 39). The variables in the excess term (${}^{o}L$ and ${}^{1}L$) are adjusted to fit experimental observations for a real solution, which generally show deviations from ideality.

The $YO_{1.5}$-ZrO_2 system description can be simplified by introducing a miscibility gap in the cubic phase field. This will be discussed in the next section. It follows that the ${}^{o}L$ and ${}^{1}L$ parameters need to be adjusted to create this feature. This is illustrated in figure 12. A single zero order term (regular solution) can only yield a symmetric miscibility gap. The ${}^{1}L$ term is also needed to produce an asymmetric miscibility gap. The effect of the sign of ${}^{1}L$ on the location of the miscibility gap is shown in figure 12 and table V. For the cubic phase in a $REO_{1.5}$-ZrO_2 phase diagram, we want the miscibility gap on the ZrO_2-rich side. This requires a positive ${}^{1}L$ and a negative second term in equation (19), which gives a second minima on the right, but less than the first minima on the left, as shown in figure 12.

The interaction parameters for the five solid solutions in this system are thus determined by (a) Using the assessment of Du (1) as a guide and (b) Estimating numbers which give a $^{ex}G_m$ which will lead to phase regions similar to those observed in the experimental phase diagram.

III.A. Cubic Solid Solution (Cubic ZrO_2 ss and Cubic $REO_{1.5}$ ss)

A major feature of the ZrO_2-Rare Earth Oxide phase diagrams is the large cubic phase field. This is evident in each of the experimental phase diagrams (figs. 1 to 4).

As pointed out by Degtyarev and Voronin (refs. 12 and 13), most of the Y_2O_3-ZrO_2 phase diagram is composed of cubic solid solutions of $YO_{1.5}$ and ZrO_2. Cubic zirconia has a classical face-centered cubic lattice CaF_2 structure. The cubic phase for Y_2O_3 has a body-centered cubic lattice like Mn_2O_3. Degtyarev and Voronin (refs. 12 and 13) further point out that this Mn_2O_3 structure can be derived from the CaF_2 structure by removing one quarter of the oxygen anions. Thus the two cubic phases can be derived from one G-x curve with a miscibility gap.

The above assumption simplifies the phase diagram calculation procedure. The miscibility gap option in Thermo-Calc is used which has the program search for a second free energy minimum. Further, the experimental phase diagrams indicate that the miscibility gap is shifted to the right.

The interaction parameters for the $YO_{1.5}$-ZrO_2 are taken from the assessment of Du et al. (ref. 1):

$$L(C,YM,ZM;\,0) = -12060 + 11.156T \tag{20}$$

$$L(C,YM,ZM;\,1) = +13784 + 5.379T \tag{21}$$

The first order interaction parameter is always positive and thus shifts the miscibility gap to the right (table V) as observed experimentally.

As shown in the database (appendix I), similar interaction parameters were taken for the $YbO_{1.5}$-ZrO_2 and $ScO_{1.5}$-ZrO_2 systems. For the $NdO_{1.5}$-ZrO_2 system, the following interaction parameters are estimated:

$$L(C,\,NM,\,ZM;\,0) = -52400 + 27T \tag{22}$$

$$L(C,\,NM,\,ZM;\,1) = +24400 + 1.5T \tag{23}$$

Again the first order interaction parameter is always positive and hence the miscibility gap is shifted to the right, as the experimental phase diagram shows. Note that equation (23) yields the similar values to equation (21) at high temperatures.

Consider the remaining interaction parameters between the various rare earth oxides. Now there is no miscibility gap and in most instances a continuous or nearly continuous cubic solution (figs. 5 to 10). Only the Yb_2O_3-Nd_2O_3 and Y_2O_3-Nd_2O_3 systems have been established with any certainty. These interaction parameters are estimated as:

$$L(C,\,BM,\,NM;\,0) = +21425 + 2.5T \tag{24}$$

$$L(C,\,BM,\,NM;\,1) = -19600 + 8T \tag{25}$$

$$L(C,\,NM,\,YM;\,0) = +21425 + 2.5T \tag{26}$$

$$L(C,\,NM,\,YM;\,1) = -19600 + 8T \tag{27}$$

The other rare earth oxide phase diagrams (Sc_2O_3–Y_2O_3, Sc_2O_3–Nd_2O_{31}, Yb_2O_3–Sc_2O_3, Yb_2O_3–Y_2O_3) are only very approximately known (figs. 5, 6, 8, and 10, respectively). In this case only the zero order interaction parameter is estimated to be +20,000 J/mol.

III.B. Hexagonal Solid Solution (Hex $REO_{1.5}$ ss)

As shown in figures 1(a) and (b), the hexagonal solid solution only occupies a small region of the Y_2O_3-ZrO_2 phase diagram. The assessment of Du et al., gives a single Redlich-Kister term:

$$L(H, YM, ZM; 0) = 50420 \tag{28}$$

As shown in figure 12, a large positive value of ^0L gives a symmetric free energy of mixing with two small minima on either side. The minima on the $YO_{1.5}$ side gives the small hexagonal region in the phase diagram.

Most of the other hexagonal ^0L solution terms were estimated to 20000 or 35000 J/mol. However the phase diagrams for the Nd_2O_3-Y_2O_3 and Nd_2O_3-Yb_2O_3 have been reported (figs. 7 and 9, respectively). In order to obtain the hexagonal solid solutions across these phase diagrams, the following expressions are used:

$$L(H, BM, NM; 0) = 12750 + 1.5T \tag{29}$$

$$L(H, BM, NM; 1) = -1000 - T \tag{30}$$

$$L(H, YM, NM; 0) = 11265 + 1.5T \tag{31}$$

$$L(H, YM, NM; 1) = 1000 - T \tag{32}$$

Both these sets of values for the interaction parameters give a free energy with a single, broad minima at the temperatures of interest.

III.C. Liquid Solution

The liquid solution parameters for the $YO_{1.5}$-ZrO_2 system have been determined by Du et al., (ref. 1) to be:

$$L(LIQ, YM, ZM; 0) = -183751 + 72.4T \tag{33}$$

$$L(LIQ, YM, ZM; 1) = 48733 - 9.476T \tag{34}$$

Due to similarity between the liquid regions in the $YO_{1.5}$-ZrO_2 and $YbO_{1.5}$-ZrO_2 systems, these same parameters are taken:

$$L(LIQ, BM, ZM; 0) = -183750 + 72.4T \tag{35}$$

$$L(LIQ, BM, ZM; 1) = 48700 - 9.48T \tag{36}$$

For the $NdO_{1.5}$-ZrO_2 system, a single term expression is used:

$$L(LIQ, NM, ZM; 0) = -20000 \tag{37}$$

$$L(LIQ, NM, ZM; 1) = -15000 \tag{38}$$

All of the $ScO_{1.5}$ parameters were estimated to 20000 J/mol. As shown in figures 3, 6, 8, and 10, virtually nothing is known about the liquid phase in the scandia systems. Thus, it is reasonable to use the above approximations.

For the other systems, zero order parameters are estimated as:

$$L(LIQ, BM, NM; 0) = -200 \tag{39}$$

$$L(LIQ, BM, YM; 0) = -10000 \tag{40}$$

$$L(LIQ, NM, YM; 0) = -200 \tag{41}$$

III.D. Monoclinic Phase Solid Solution (Mon ZrO_2 ss)

The monoclinic phases show very limited solubility for a second oxide, except for the $NdO_{1.5}$-$YbO_{1.5}$ and $NdO_{1.5}$-$YO_{1.5}$ systems. Again, beginning with the data from the assessment of Du et al., (ref. 1):

$$L(M, YM, ZM; 0) = -58223 + 98.126T \tag{42}$$

The other interaction parameters are estimated. Only two terms are used for the $NdO_{1.5}$-$YbO_{1.5}$ and $NdO_{1.5}$-$YO_{1.5}$ systems:

$$L(M, BM, NM; 0) = -5000 \tag{43}$$

$$L(M, BM, NM; 1) = 100 \tag{44}$$

$$L(M, NM, YM; 0) = -50000 \tag{45}$$

$$L(M, NM, YM; 1) = 1000 \tag{46}$$

The remaining zero order interaction parameters are all estimated to be 20000 J/mol.

IIII.E. Phase MN Solid Solution (MN ss)

Again, since only the $YbO_{1.5}$-$NdO_{1.5}$ and $YO_{1.5}$-$NdO_{1.5}$ phase diagrams are known with any certainty, these interaction parameters are taken as:

$$L(MN, BM, NM; 0) = -160000 + 48T \tag{47}$$

$$L(MN, BM, NM; 1) = 120000 - 15T \tag{48}$$

$$L(MN, NM, YM; 0) = -160000 + 50T \tag{49}$$

$$L(MN, NM, YM: 1) = 120000 + 15T \tag{50}$$

All other interaction parameters are taken as 20000 J/mol.

III.F. N Phase Solid Solution (N ss)

As above, since only the $YbO_{1.5}$-$NdO_{1.5}$ and $YO_{1.5}$-$NdO_{1.5}$ phase diagrams are known with any certainty, these interaction parameters are taken as:

$$L(N, BM, NM; 0) = -15200 - 7T \tag{51}$$

$$L(N, BM, NM; 1) = -13000 - 6.7T \tag{52}$$

$$L(N, NM, YM; 0) = -15000 - 7T \tag{53}$$

$$L(N, NM, YM; 1) = 13000 + 5T \tag{54}$$

All other interaction parameters are taken as 20000 J/mol, except for:

$$L(N, NM, ZM; 0) = 50000 \tag{55}$$

III.G. Tetragonal Phase Solid Solution (Tet ZrO_2 ss)

This phase shows a triangular appearance in the Y_2O_3-ZrO_2 phase diagram (figs. 1(a) and (b)). There is a suggestion on the other RE_2O_3-ZrO_2 phase diagrams (figs. 2 to 4) of similar behavior. The assessment of Du et al., (1) gives:

$$L(T, YM, ZM; 0) = -25800 \tag{56}$$

The same value is adopted for $YbO_{1.5}$-$ZrO_{1.5}$:

$$L(T, BM, ZM; 0) = -25800 \tag{57}$$

All other interaction parameters are estimated to be 20000 J/mol.

IV. INTERMEDIATE COMPOUNDS

In the binary $NdO_{1.5}$-ZrO_2, $ScO_{1.5}$-ZrO_2, and $YbO_{1.5}$-ZrO_2 systems there are several intermediate compounds. The $Zr_3Y_4O_{12}$ phase has been reported by several investigators. These line compounds are treated with two sublattice model—the ZrO_2 component is on one sublattice and the $YO_{1.5}$ component is one the other sublattice. Following Du et al.:

$$G_{(1/7)Zr_3Y_4O_{12}} = \frac{3}{7}\ {}^0G^{C-ZrO_2} + \frac{4}{7}\ {}^0G^{C'-ZrO_2} - 3284.3 - 2.26749T = -79536 + 24.72T \tag{58}$$

As mentioned, there is an analogous $Zr_3Yb_4O_{12}$ phase. This is treated as:

$$G_{(1/7)Zr_3Yb_4O_{12}} = -79350 + 25T \tag{59}$$

To account for interchange of Y and Yb in this compound, the following solution parameter is introduced:

$$L(DELTA,BM,YM{:}ZM;0) = 10200 \tag{60}$$

The free energy of each of the compounds are chosen so that they protrude into the cubic phase. For $NdO_{1.5}$-ZrO_2, there exists a binary with the 1:1 composition

$$G(P, NM{:}\ ZM; 0) = -180450 + 57T \tag{61}$$

For the $ScO_{1.5}$-ZrO_2, there are several intermediate compounds, each with a range of solution according to the experimental diagram in figure 3. However for the purpose of this approximation, we shall treat them as line compounds.

For $4(ScO_{1.5}) \cdot 3(ZrO_2)$, Phase RB:

$$G(RB, SM{:}\ ZM; 0) = -557200 + 171.5T \tag{62}$$

For $2(ScO_{1.5}) \cdot 5(ZrO_2)$, Phase RH:

$$G(RH, SM{:}\ ZM; 0) = -620000 + 185T \tag{63}$$

For $2(ScO_{1.5}) \cdot 7(ZrO_2)$, Phase RM:

$$G(RM, SM{:}\ ZM; 0) = -822800 + 258T \tag{64}$$

V. RESULTS: BINARY PHASE DIAGRAMS

Having described the database, we now turn to the results for the binaries and compare them to the limited experimental data. Figures 13 to 22 give the calculated binaries. Recall again that the experimental diagrams are for RE_2O_3-ZrO_2 whereas the calculated diagrams are for $REO_{1.5}$- ZrO_2.

The calculated diagrams show the same general features as the experimental diagrams. The calculated $YO_{1.5}$-ZrO_2 phase diagram (fig. 13) is, of course, the same as that obtained by Du et al., (ref. 1) and is in good agreement with the experimental diagram of Stubican et al., (fig. 1(a)).

All other $REO_{1.5}$-ZrO_2 diagrams show similar behavior to the $YO_{1.5}$-ZrO_2 phase diagram on the ZrO_2-rich side, where most of the interest is. The $NdO_{1.5}$-ZrO_2, $ScO_{1.5}$-ZrO_2, and $YbO_{1.5}$-ZrO_2 diagrams are not so definitive, as much less experimental data is available. Nonetheless, the general features of the experimental diagrams are reproduced on the calculated diagrams.

The Yb_2O_3-ZrO_2 diagram is also only approximately known (fig. 2) and consists of a large cubic phase field and one intermediate compound. This is reproduced in the calculated diagram (fig. 14).

The Nd_2O_3-ZrO_2 experimental diagram shows a eutectic at ~2115 °C and the $NdO_{1.5}$-ZrO_2 calculated diagram shows the same eutectic at 2100 °C. The Nd_2O_3-ZrO_2 experimental diagram shows a euctectoid at 1440 °C, whereas the calculated $NdO_{1.5}$-ZrO_2 phase diagram shows this eutectoid at ~1660 °C. But this part of the diagram is not well-known.

Only a limited portion of the Sc_2O_3-ZrO_2 phase diagram is known (fig. 3). For the purpose of this approximation, the intermediate compounds ($Sc_2Zr_7O_{17}$, $Sc_2Zr_5O_{13}$, $Sc_4Zr_3O_{12}$) are treated as line compounds rather than solid solutions. Even with this approximation, the general appearance is reproduced.

For the binaries among the rare earth oxides (Nd_2O_3, Sm_2O_3, Yb_2O_3, Y_2O_3), only the Nd_2O_3-Y_2O_3 (fig. 7) and Nd_2O_3-Yb_2O_3 (fig. 9) systems are known to any extent. The major features of these diagrams are reproduced in the calculated diagrams (figs. 19 and 21, respectively). Both show a substantial monoclinic solid solution. The remaining rare earth oxide binaries show large cubic solid solution regions.

There are some limited activity measurements for the Y_2O_3-ZrO_2 system at 2773 K (ref. 40) and the Sc_2O_3-ZrO_2 system at 2600 K (ref. 41) obtained via mass spectrometry. In order to compare these data to calculations from the database described here, the mole fraction must be converted according to table IV and the activity also must be converted to appropriate units. Belov et al. (refs. 40 and 41) show that the rare earth oxides vaporize as:

$$RE_2O_3(s) = 2\,REO(g) + O(g) \tag{65}$$

Thus the activity of RE_2O_3 [$a(RE_2O_3)$] is defined as:

$$a(RE_2O_3) = \frac{[P(REO)]^2[P(O)]}{[P^o(REO)]^2[P^o(O)]} \tag{66}$$

Here the quantities in the numerator are the partial pressures over the oxide in solution and the quantities in the denominator are the partial pressures over the pure oxide—solid Y_2O_3 (presumably hexagonal) and cubic Sc_2O_3.

Next consider $REO_{1.5}$, which should vaporize as:

$$REO_{1.5}(s) = REO(g) + \tfrac{1}{2}\,O(g) \tag{67}$$

$$a(REO_{1.5}) = \frac{[P(REO)][P(O)]^{1/2}}{[P^o(REO)][P^o(O)]^{1/2}} = \sqrt{a(RE_2O_3)} \tag{68}$$

Thus the experimental measurements need only be converted with a square root for comparison to the calculated values.

Figures 23(a and b) and 24(a and b) show the comparison of these measured activities (refs. 40 and 41) to the calculated values from this database. For both systems the data indicate measurements were taken in a single phase region across the diagram; whereas the phase diagrams—both experiment and calculated indicate some two phase regions. There appears to be a conflict in the phase boundary locations. Agreement with $a(ZrO_2)$ is good, as these data were used in the Du et al. (ref. 1) assessment. However, agreement with $a(REO_{1.5})$ is only fair—these data were not used in the assessment.

VI. RESULTS: TERNARY SECTIONS

This database can be used to approximate ternary sections. One would expect the following features in a ternary diagram:

1. The cubic phase occupies a large region in each binary. Therefore it seems reasonable that the cubic phase would stretch across the ternary as well.
2. The intermediate compounds should protrude into the ternary.

Calculations of the isothermal cuts led to some convergence problems in ThermoCalc and additional steps were necessary to force convergence. These are illustrated in the macro in appendix II. This macro also allows the variation of the ternary interaction parameter.

Figures 25(a) and (b) are isothermal cuts for the $YO_{1.5}$-$YbO_{1.5}$-ZrO_2 system at 1600 K, illustrating the effects of two different ternary interaction parameters:

Figure 24(a): L(C, BM, YM, ZM; 0) = +10000, insufficient for a continuous two phase region.

Figure 24(b): L(C, BM, YM, ZM; 0) = +100000, continuous two phase region.

In order to address issue (2) above, an interaction parameter was added for the intermediate phase. Figure 25 shows the effect of

L(C, BM, YM: ZM) = 70000

L(DELTA, BM, YM: ZM) = 10200

Figures 26(a) to (c) are the calculated ternary for 1473, 1673, and 2000 K. These can be compared to experimental sections in figure 11. The protrusion behavior as a function of temperature for the delta phase is reproduced by these calculations. Further work is necessary to reproduce the phase boundaries of the solution phases correctly.

VI. RESULTS: HIGHER ORDER SYSTEMS

There are no reported data on higher order phase diagrams. However they can be approximated with this database. Phase data for systems with more than three components can be presented with a phase fraction diagram or an isoplethal section with one component varying over a small range. An example of a phase fraction diagram for $ScO_{1.5}$-$YO_{1.5}$-$YbO_{1.5}$-ZrO_2 is shown in figure 27. Figure 28 shows an isoplethal section for $ScO_{1.5}$-$YO_{1.5}$-$YbO_{1.5}$-ZrO_2 with a small variation in $YO_{1.5}$.

VII. SUMMARY AND CONCLUSIONS

An approximate database for $ScO_{1.5}$-$NdO_{1.5}$-$YbO_{1.5}$-$YO_{1.5}$-ZrO_2 has been discussed. It is based on the assessment of Du et al., for the $YO_{1.5}$-ZrO_2 system (ref. 1) and uses a two-term lattice stability description of the phases with the liquid as the reference state. Binary phase diagrams for the other systems agree reasonably well with the limited experimental data. Ternary and higher order diagrams require the introduction of a ternary interaction parameter and an interaction parameter for the intermediate compounds to allow protrusion of the intermediate compounds into the multi-component composition space. The binary systems beyond Y_2O_3-ZrO_2 require additional experimental and modeling efforts. This will provide a stronger basis for further development of the multicomponent diagrams.

APPENDIX I

```
$ Database file written 99-12-23
$
 ELEMENT /-   ELECTRON_GAS              0.0000E+00  0.0000E+00  0.0000E+00!
 ELEMENT VA   VACUUM                    0.0000E+00  0.0000E+00  0.0000E+00!
 ELEMENT BM   LIQ                       1.9704E+02  0.0000E+00  0.0000E+00!
 ELEMENT NM   LIQ                       1.6827E+02  0.0000E+00  0.0000E+00!
 ELEMENT SM   LIQ                       6.8960E+01  0.0000E+00  0.0000E+00!
 ELEMENT YM   LIQ                       1.1291E+02  0.0000E+00  0.0000E+00!
 ELEMENT ZM   LIQ                       1.2322E+02  0.0000E+00  0.0000E+00!

 FUNCTION UN_ASS     2.98140E+02  0.0 ;  3.00000E+02  N !

 TYPE_DEFINITION % SEQ *!
 DEFINE_SYSTEM_DEFAULT SPECIE 2 !
 DEFAULT_COMMAND DEF_SYS_ELEMENT VA !


 PHASE C  %  1  1.0  !
    CONSTITUENT C  :BM,NM,SM,YM,ZM :  !

   PARAMETER G(C,BM;0)  5.00000E+02  -65942+25.105*T;  6.00000E+03  N REF:0 !
   PARAMETER G(C,NM;0)  5.00000E+02  -65348+25.105*T;  6.00000E+03  N REF:0 !
   PARAMETER G(C,SM;0)  5.00000E+02  -67856+25.105*T;  6.00000E+03  N REF:0 !
   PARAMETER G(C,YM;0)  5.00000E+02  -67419+25.105*T;  6.00000E+03  N REF:0 !
   PARAMETER G(C,ZM;0)  5.00000E+02  -87987+29.496*T;  6.00000E+03  N REF:0 !
   PARAMETER G(C,BM,NM;0)  5.00000E+02  +21425-2.5*T;  6.00000E+03  N REF:0 !
   PARAMETER G(C,BM,NM;1)  5.00000E+02  -19600+8*T;  6.00000E+03  N REF:0 !
   PARAMETER G(C,BM,SM;0)  5.00000E+02  20000;  6.00000E+03  N REF:0 !
   PARAMETER G(C,BM,YM;0)  5.00000E+02  20000;  6.00000E+03  N REF:0 !
   PARAMETER G(C,BM,ZM;0)  5.00000E+02  -12060+11.16*T;  6.00000E+03  N
  REF:0 !
   PARAMETER G(C,BM,YM,ZM) 300          +70000; 6000 N REF: 0 !
   PARAMETER G(C,BM,ZM;1)  5.00000E+02  +13800+5.38*T;  6.00000E+03  N REF:0 !
   PARAMETER G(C,NM,SM;0)  5.00000E+02  20000;  6.00000E+03  N REF:0 !
   PARAMETER G(C,NM,YM;0)  5.00000E+02  +21425-2.5*T;  6.00000E+03  N REF:0 !
   PARAMETER G(C,NM,YM;1)  5.00000E+02  +19600-8*T;  6.00000E+03  N REF:0 !
   PARAMETER G(C,NM,ZM;0)  5.00000E+02  -52400+27*T;  6.00000E+03  N REF:0 !
   PARAMETER G(C,NM,ZM;1)  5.00000E+02  +24400+1.5*T;  6.00000E+03  N REF:0 !
   PARAMETER G(C,SM,YM;0)  5.00000E+02  20000;  6.00000E+03  N REF:0 !
   PARAMETER G(C,SM,ZM;0)  5.00000E+02  -12000+11*T;  6.00000E+03  N REF:0 !
   PARAMETER G(C,SM,ZM;1)  5.00000E+02  +14500+6*T;  6.00000E+03  N REF:0 !
   PARAMETER G(C,YM,ZM;0)  5.00000E+02  -12060+11.156*T;  6.00000E+03  N
  REF:0 !
   PARAMETER G(C,YM,ZM;1)  5.00000E+02  +13784+5.379*T;  6.00000E+03  N
  REF:0 !


 PHASE DELTA  %  2 .571   .429 !
    CONSTITUENT DELTA  :BM,YM : ZM :  !

   PARAMETER G(DELTA,YM:ZM;0)  5.00000E+02  -79536+24.72*T;  6.00000E+03  N
  REF:0 !
   PARAMETER G(DELTA,BM:ZM;0)  300    -79350+25*T; 6000 N REF:0 !
   PARAMETER G(DELTA,BM,YM:ZM;0) 300  +10200; 6000 N REF: 0 !
```

```
PHASE H  %  1  1.0  !
   CONSTITUENT H  :BM,NM,SM,YM,ZM :  !

  PARAMETER G(H,BM;0)  2.98150E+02  -55919+20.92*T;   6.00000E+03   N REF:0 !
  PARAMETER G(H,NM;0)  2.98150E+02  -75697+29.29*T;   6.00000E+03   N REF:0 !
  PARAMETER G(H,SM;0)  2.98150E+02  -54000+30*T;   6.00000E+03   N REF:0 !
  PARAMETER G(H,YM;0)  5.00000E+02  -56735+20.92*T;  6.00000E+03  N REF:0 !
  PARAMETER G(H,ZM;0)  5.00000E+02  -53973+25.104*T;  6.00000E+03  N REF:0 !
  PARAMETER G(H,BM,NM;0)  5.00000E+02  +12750+1.5*T;  6.00000E+03  N REF:0 !
  PARAMETER G(H,BM,NM;1)  5.00000E+02  -1000-T;  6.00000E+03  N REF:0 !
  PARAMETER G(H,BM,SM;0)  5.00000E+02  20000;  6.00000E+03  N REF:0 !
  PARAMETER G(H,BM,YM;0)  5.00000E+02  +20000;  6.00000E+03  N REF:0 !
  PARAMETER G(H,BM,ZM;0)  5.00000E+02  20000;  6.00000E+03  N REF:0 !
  PARAMETER G(H,NM,SM;0)  5.00000E+02  20000;  6.00000E+03  N REF:0 !
  PARAMETER G(H,NM,YM;0)  5.00000E+02  +11265+1.5*T;  6.00000E+03  N REF:0 !
  PARAMETER G(H,NM,YM;1)  5.00000E+02  +1000+T;  6.00000E+03  N REF:0 !
  PARAMETER G(H,NM,ZM;0)  5.00000E+02  35000;  6.00000E+03  N REF:0 !
  PARAMETER G(H,SM,YM;0)  5.00000E+02  20000;  6.00000E+03  N REF:0 !
  PARAMETER G(H,SM,ZM;0)  5.00000E+02  20000;  6.00000E+03  N REF:0 !
  PARAMETER G(H,YM,ZM;0)  5.00000E+02  50420;  6.00000E+03  N REF:0 !


 PHASE LIQ  %  1  1.0  !
   CONSTITUENT LIQ  :BM,NM,SM,YM,ZM :  !

      PARA G(LIQ,BM;0) 298.15 0; 6000 N!
      PARA G(LIQ,NM;0) 298.15 0; 6000 N!
      PARA G(LIQ,SM;0) 298.15 0; 6000 N!
      PARA G(LIQ,YM;0) 298.15 0; 6000 N!
      PARA G(LIQ,ZM;0) 298.15 0; 6000 N!
  PARAMETER G(LIQ,BM,NM;0)  5.00000E+02  -200;  6.00000E+03  N REF:0 !
  PARAMETER G(LIQ,BM,SM;0)  5.00000E+02  20000;  6.00000E+03  N REF:0 !
  PARAMETER G(LIQ,BM,YM;0)  5.00000E+02  -10000;  6.00000E+03  N REF:0 !
  PARAMETER G(LIQ,BM,ZM;0)  5.00000E+02  -183750+72.4*T;  6.00000E+03  N
 REF:0 !
  PARAMETER G(LIQ,BM,ZM;1)  5.00000E+02  +48700-9.48*T;  6.00000E+03  N
 REF:0 !
  PARAMETER G(LIQ,NM,SM;0)  5.00000E+02  20000;  6.00000E+03  N REF:0 !
  PARAMETER G(LIQ,NM,YM;0)  5.00000E+02  -200;  6.00000E+03  N REF:0 !
  PARAMETER G(LIQ,NM,ZM;0)  5.00000E+02 -20000;  6.00000E+03  N REF:0 !
  PARAMETER G(LIQ,NM,ZM;1)  500         -15000; 6000  N REF: 0 !
  PARAMETER G(LIQ,SM,YM;0)  5.00000E+02  20000;  6.00000E+03  N REF:0 !
  PARAMETER G(LIQ,SM,ZM;0)  5.00000E+02  20000;  6.00000E+03  N REF:0 !
  PARAMETER G(LIQ,YM,ZM;0)  5.00000E+02  -183751+72.4*T;  6.00000E+03  N
 REF:0 !
  PARAMETER G(LIQ,YM,ZM;1)  5.00000E+02  +48733-9.476*T;  6.00000E+03  N
 REF:0 !


 PHASE M  %  1  1.0  !
   CONSTITUENT M  :BM,NM,SM,YM,ZM :  !

  PARAMETER G(M,BM;0)  5.00000E+02  -14000+29.915*T;  6.00000E+03  N REF:0 !
  PARAMETER G(M,NM;0)  5.00000E+02  -14000+29.915*T;  6.00000E+03  N REF:0 !
  PARAMETER G(M,SM;0)  5.00000E+02  -14000+29.915*T;  6.00000E+03  N REF:0 !
  PARAMETER G(M,YM;0)  5.00000E+02  -14698+29.915*T;  6.00000E+03  N REF:0 !
  PARAMETER G(M,ZM;0)  5.00000E+02  -99979+35.9*T;  6.00000E+03  N REF:0 !
```

```
  PARAMETER G(M,BM,NM;0)  5.00000E+02 -5000;  6.00000E+03  N REF:0 !
  PARAMETER G(M,BM,NM;1)  5.00000E+02  100;  6.00000E+03  N REF:0 !
  PARAMETER G(M,BM,SM;0)  5.00000E+02  20000;  6.00000E+03  N REF:0 !
  PARAMETER G(M,BM,YM;0)  5.00000E+02  20000;  6.00000E+03  N REF:0 !
  PARAMETER G(M,BM,ZM;0)  5.00000E+02  20000;  6.00000E+03  N REF:0 !
  PARAMETER G(M,NM,SM;0)  5.00000E+02  20000;  6.00000E+03  N REF:0 !
  PARAMETER G(M,NM,YM;0)  5.00000E+02  -50000;  6.00000E+03  N REF:0 !
  PARAMETER G(M,NM,YM;1)  5.00000E+02  1000;  6.00000E+03  N REF:0 !
  PARAMETER G(M,NM,ZM;0)  5.00000E+02  20000;  6.00000E+03  N REF:0 !
  PARAMETER G(M,SM,YM;0)  5.00000E+02  20000;  6.00000E+03  N REF:0 !
  PARAMETER G(M,SM,ZM;0)  5.00000E+02  20000;  6.00000E+03  N REF:0 !
  PARAMETER G(M,YM,ZM;0)  5.00000E+02  -58223+98.126*T;  6.00000E+03  N
 REF:0 !

PHASE MN  %  1  1.0  !
   CONSTITUENT MN  :BM,NM,SM,YM,ZM :  !

  PARAMETER G(MN,BM;0)  5.00000E+02  -45000+30*T;  6.00000E+03  N REF:0 !
  PARAMETER G(MN,NM;0)  5.00000E+02  -60000+30*T;  6.00000E+03  N REF:0 !
  PARAMETER G(MN,SM;0)  5.00000E+02  -60000+30*T;  6.00000E+03  N REF:0 !
  PARAMETER G(MN,YM;0)  5.00000E+02  -45000+30*T;  6.00000E+03  N REF:0 !
  PARAMETER G(MN,ZM;0)  5.00000E+02  -45000+30*T;  6.00000E+03  N REF:0 !
  PARAMETER G(MN,BM,NM;0)  5.00000E+02  -160000+48*T;  6.00000E+03  N REF:0 !
  PARAMETER G(MN,BM,NM;1)  5.00000E+02  +120000-15*T;  6.00000E+03  N REF:0 !
  PARAMETER G(MN,BM,SM;0)  5.00000E+02  20000;  6.00000E+03  N REF:0 !
  PARAMETER G(MN,BM,YM;0)  5.00000E+02  20000;  6.00000E+03  N REF:0 !
  PARAMETER G(MN,BM,ZM;0)  5.00000E+02  20000;  6.00000E+03  N REF:0 !
  PARAMETER G(MN,NM,SM;0)  5.00000E+02  20000;  6.00000E+03  N REF:0 !
  PARAMETER G(MN,NM,YM;0)  5.00000E+02  -160000+50*T;  6.00000E+03  N REF:0 !
  PARAMETER G(MN,NM,YM;1)  5.00000E+02  -120000+15*T;  6.00000E+03  N REF:0 !
  PARAMETER G(MN,NM,ZM;0)  5.00000E+02  20000;  6.00000E+03  N REF:0 !
  PARAMETER G(MN,SM,YM;0)  5.00000E+02  20000;  6.00000E+03  N REF:0 !
  PARAMETER G(MN,SM,ZM;0)  5.00000E+02  20000;  6.00000E+03  N REF:0 !
  PARAMETER G(MN,YM,ZM;0)  5.00000E+02  20000;  6.00000E+03  N REF:0 !

PHASE N  %  1  1.0  !
   CONSTITUENT N  :BM,NM,SM,YM,ZM :  !

  PARAMETER G(N,BM;0)  5.00000E+02  -50000+30*T;  6.00000E+03  N REF:0 !
  PARAMETER G(N,NM;0)  5.00000E+02  -78000+30.29*T;  6.00000E+03  N REF:0 !
  PARAMETER G(N,SM;0)  5.00000E+02  -50000+30*T;  6.00000E+03  N REF:0 !
  PARAMETER G(N,YM;0)  5.00000E+02  -50000+30*T;  6.00000E+03  N REF:0 !
  PARAMETER G(N,ZM;0)  5.00000E+02  -50000+30*T;  6.00000E+03  N REF:0 !
  PARAMETER G(N,BM,NM;0)  5.00000E+02 -15200-7*T; 6000  N REF:0 !
  PARAMETER G(N,BM,NM;1)  500         -13000-6.7*T;  6000  N REF:0!
  PARAMETER G(N,BM,SM;0)  5.00000E+02  20000;  6.00000E+03  N REF:0 !
  PARAMETER G(N,BM,YM;0)  5.00000E+02  20000;  6.00000E+03  N REF:0 !
  PARAMETER G(N,BM,ZM;0)  5.00000E+02  20000;  6.00000E+03  N REF:0 !
  PARAMETER G(N,NM,SM;0)  5.00000E+02  20000;  6.00000E+03  N REF:0 !
  PARAMETER G(N,NM,YM;0)  500       -15000-7*T;  6.00000E+03  N REF:0 !
  PARAMETER G(N,NM,YM;1)  500         13000+5*T; 6000 N REF: 0 !
  PARAMETER G(N,NM,ZM;0)  5.00000E+02  50000;  6.00000E+03  N REF:0 !
  PARAMETER G(N,SM,YM;0)  5.00000E+02  20000;  6.00000E+03  N REF:0 !
  PARAMETER G(N,SM,ZM;0)  5.00000E+02  20000;  6.00000E+03  N REF:0 !
  PARAMETER G(N,YM,ZM;0)  5.00000E+02  20000;  6.00000E+03  N REF:0 !
```

```
PHASE P  %  2 1   1 !
   CONSTITUENT P  :NM : ZM :  !

  PARAMETER G(P,NM:ZM;0)  5.00000E+02  -180450+57*T;  6.00000E+03  N REF:0 !


PHASE RB  %  2 4   3 !
   CONSTITUENT RB  :SM : ZM :  !

  PARAMETER G(RB,SM:ZM;0)  5.00000E+02  -557200+171.5*T;  6.00000E+03  N
 REF:0 !


PHASE RH  %  2 2   5 !
   CONSTITUENT RH  :SM : ZM :  !

  PARAMETER G(RH,SM:ZM;0)  5.00000E+02  -620000+185*T;  6.00000E+03  N
 REF:0 !


PHASE RM  %  2 2   7 !
   CONSTITUENT RM  :SM : ZM :  !

  PARAMETER G(RM,SM:ZM;0)  5.00000E+02  -822800+258*T;  6.00000E+03  N
 REF:0 !


PHASE T  %  1  1.0  !
   CONSTITUENT T  :BM,NM,SM,YM,ZM :  !

  PARAMETER G(T,BM;0)  5.00000E+02  -35000+26.462*T;  6.00000E+03  N REF:0 !
  PARAMETER G(T,NM;0)  5.00000E+02  -35000+26.462*T;  6.00000E+03  N REF:0 !
  PARAMETER G(T,SM;0)  5.00000E+02  -35000+26.462*T;  6.00000E+03  N REF:0 !
  PARAMETER G(T,YM;0)  5.00000E+02  -35618+26.462*T;  6.00000E+03  N REF:0 !
  PARAMETER G(T,ZM;0)  5.00000E+02  -93955+31.755*T;  6.00000E+03  N REF:0 !
  PARAMETER G(T,BM,NM;0)  5.00000E+02  20000;  6.00000E+03  N REF:0 !
  PARAMETER G(T,BM,SM;0)  5.00000E+02  20000;  6.00000E+03  N REF:0 !
  PARAMETER G(T,BM,YM;0)  5.00000E+02  20000;  6.00000E+03  N REF:0 !
  PARAMETER G(T,BM,ZM;0)  5.00000E+02  -25800;  6.00000E+03  N REF:0 !
  PARAMETER G(T,NM,SM;0)  5.00000E+02  20000;  6.00000E+03  N REF:0 !
  PARAMETER G(T,NM,YM;0)  5.00000E+02  20000;  6.00000E+03  N REF:0 !
  PARAMETER G(T,NM,ZM;0)  5.00000E+02  20000;  6.00000E+03  N REF:0 !
  PARAMETER G(T,SM,YM;0)  5.00000E+02  20000;  6.00000E+03  N REF:0 !
  PARAMETER G(T,SM,ZM;0)  5.00000E+02  20000;  6.00000E+03  N REF:0 !
  PARAMETER G(T,YM,ZM;0)  5.00000E+02  -25800;  6.00000E+03  N REF:0 !


LIST_OF_REFERENCES
NUMBER  SOURCE
 !
```

APPENDIX II

```
$ MACRO bmymzm-3.tcm GENERATED ON PC/WINDOWS NT    DATE  0- 3- 8
$ Make the BM-YM-ZM ternary with a L(C,BM,YM,ZM;0) term directly
$

go da
sw user nasa5r1
def-sys bm ym zm
get

go gib
l-p-d
c
ent-par

L
C
bm
ym
zm

0
500
@? Enter Value

6000
N

l-p-d
c

go p-3
sp-op
SET_MISCIBILITY_GAP
c
2
bm ym

s-c n=1, t=1600, p=1e5, x(ym)=.78, x(zm)=.219
l-c
c-e

s-a-s
N
Y
zm
Y
bm ym
N
N
bm
N
bm
N
```

```
bm
N
bm
N
bm
N
bm

s-c n=1, t=1600, p=1e5, x(ym)=.78, x(zm)=.219
l-c
c-e *
l-e
SCREEN
VWCS
s-a-v 1 x(ym)
0
1
.025
s-a-v 2 x(zm)
0
1
.025
add
-1
li-in-eq
save
bmymzm-3
y
map
post
s-d-t
y
Y
n
pl
SCREEN
ba
read
bmymzm-3.PL3
l-c
s-c x(ym)=1e-3, x(zm)=.21
l-c
c-e *
c-e
l-e
SCREEN
VWCS
add
2
li-in-eq
s-c x(ym)=.05, x(zm)=.9
l-c
c-e
c-e
l-e
SCREEN
VWCS
```

```
add
-2
li-in-eq
save
bmymzm-3.PL3
y
map
post
s-t-s
4
s-c-t L_L
YbO1.5
s-c-t l-r
YO1.5
s-c-t t
ZrO2
s-f
4
0.3
s-a-t-s
x
N
X(YO1.5)
s-a-t-s
Y
N
X(ZrO2)
s-tit
YbO1.5-YO1.5-ZrO2 1600K
s-l-c
n
pl
SCREEN
dump
bmp
ba
read bmymzm-3.PL3
li-in-eq
s-c x(ym)=0.78, x(zm)=0.21
l-c
c-e *

l-e

add
-1
save
bmymzm-3.PL3
y
map
post
pl
SCREEN
set-int
ba
```

REFERENCES

1. Y. Du, Z. Jin, and P. Huang, "Thermodynamic Assessment of the ZrO_2-$YO_{1.5}$ System," J. Am. Ceram. Soc. 74 [7] pp. 1569–77 (1991).
2. P. Duwez, F.H. Brown, Jr., and Odell, F., "The Zirconia-Yttria System," J. Electrochem. Soc. 98, pp. 356–62 (1951).
3. T. Noguchi, M. Mizuno, and T. Yamada, "The Liquidus Curve of the ZrO_2-Y_2O_3 System as Measured by a Solar Furnace," Bull. Chem. Soc. Japan 43, pp. 2614–16 (1970).
4. S.R. Skaggs, "The Zirconia-Yttria System above 2000 °C," PhD Dissertation, University of New Mexico, Albuquerque, New Mexico, 1972.
5. K.K. Srivastava, R.N. Patil, C.B. Choudhary, K.V.G.K. Gokhale, and E.C. Subbaro, "Revised Phase Diagram of the System ZrO_2-$YO_{1.5}$," Trans. J. Brit. Ceram. Soc. 73 [2], pp. 85–91 (1974).
6. H.G. Scott, "Phase relationships in the zirconia-yttria system," J. Mat. Sci. 10, pp. 1527–35 (1975).
7. V.S. Stubican, R.C. Hink, and S.P. Ray, "Phase Equilibria and Ordering in the System ZrO_2-Y_2O_3," J. Am. Ceram. Soc. 61 [1/2], pp. 17–21 (1978).
8. V.S. Stubican and J.R. Hellman, "Phase Equilibria in some zirconia systems," in Science and Technology of Zirconia, pp. 25–36, Advances in Ceramics, Volume 3, ed. by A.H. Heuer and L. W. Hobbs, American Ceramic Society, Columbus, OH, 1981.
9. C. Pascual and P. Duran, "Subsolidus Phase Equilibria and Ordering in the System ZrO_2-Y_2O_3," J. Am. Ceram. Soc. 66 [1], pp. 23–27 (1983).
10. R. Ruh, K.S. Mazdiyasni, P.G. Valentine, and H.O. Bielstein, "Phase Relations in the System ZrO_2-Y_2O_3 at Low Y_2O_3 Contents," J. Am. Ceram. Soc. C-190–92 (1984).
11. V.S. Stubican, G.S. Corman, J.R. Hellman, and G. Senft, "Phase Relationships in Some ZrO_2 Systems," pp. 96–106, Science and Technology of Zirconia II, Adv. in Ceramics, Vol. 12, ed. by N. Claussen, M. Ruhle, and A. H. Heuer, Am. Ceram. Soc., Columbus, OH, 1984.
12. S.A. Degtyarev and G.F. Voronin, "Solution of Incorrect Problems in the Thermodynamics of Phase Equilibria. I. The System ZrO_2-Y_2O_3," Russ. J. Phys. Chem. 61 [3], pp. 317–20 (1987).
13. S.A. Degtyarev and G.F. Voronin, "Solution of "Incorrect" Problems in the Thermodynamics of Phase Equilibria. I. Calculation of the ZrO_2-Y_2O_3 Phase Diagram," Russ. J. Phys. Chem. 61 [3], pp. 320–23 (1987).
14. L. Kaufman, "Calculation of Multicomponent Ceramic Phase Diagrams," Physica B 150, pp. 99–114 (1988).
15. Y. Du, Z. Jin, and P. Huang, "Thermodynamic Calculation of the ZrO_2-$YO_{1.5}$ System," J. Am. Ceram. Soc. 74 [9], pp. 2107–12 (1993).
16. Y. Du and Z. Jin, "Optimization and Calculation of ZrO_2-MgO System," CALPHAD, 15 [1], pp. 59–68 (1991).
17. Z. Jin and Y. Du, "A Reassessment of the ZrO_2-$YO_{1.5}$-MgO System," Ceramics Int. 20, pp. 17–25 (1994).
18. H. Yokokawa, N. Sakai, T. Kawada, and M. Dokiya, "Phase Diagram Calculations for ZrO_2 Based Ceramics: Thermodynamic Regularities in Zirconate Formation and Solubilities of Transition Metal Oxides," Science and Technology of Zirconia V,
19. H. Yokokawa, "Phase Diagrams and Thermodynamic Properties of Zirconia Based Ceramics," Key Engineering Materials, pp. 153–154, 37–74 (1998).
20. F.H. Brown, Jr. and P. Duwez, "The Systems Zirconium Oxide-Lanthanum Oxide and Zirconium Oxide-Neodymium Oxide," J. Am. Ceram. Soc. 38 [3], pp. 95–101 (1955).
21. A. Rouanet, "Zirconium Dioxide-Lanthanide Oxide Systems Close to the Melting Point," Rev. Int. Hautes Temp. Refract. 8 [2], pp. 161–80 (1971).
22. M.A. Clevinger, K.M. Hill, T.R. Green, C.C. Cedeno, E. Hayward, and N. Swanson, "Phase Equilbrium Diagrams, CD-ROM Database, Version 2.1," Am. Ceram. Soc., Westerville, OH, 1993, Figure 93–023.
23. ibid., Figure 93-055.
24. ibid., Figure 5257.
25. ibid., Figure 4430.
26. ibid., Figure 4426.
27. ibid., Figure 347.
28. ibid., Figure 351.
29. ibid., Figure 5234.
30. ibid., Figure 5235.
31. G.S. Corman and V.S. Stubican, "Phase Equilibria and Ionic Conductivity in the System- ZrO_2-Yb_2O_3-Y_2O_3," J. Am. Ceram. Soc. 68 [4], pp. 174–81 (1985).
32. H.L. Lukas, E.-Th. Henig, and B. Zimmermann, "Optimization of Phase Diagrams by a Least Squares Method Using Simultaneously Different Types of Data," CALPHAD 1 [3], pp. 2215–36 (1977).
33. O. Kubachewski and C.B. Alcock, Metallurgical Thermochemistry, 5th Edition, Pergamon Press, Oxford, 1983.

34. L.V. Gurvich, V.S. Iorish, D.V. Chekhovskoi, and V.S. Yungman, IVTANTHERMO-A Thermodynamic Database and Software System for the Personal Computer, NIST Special Database 5, NIST, Gaithersburg, MD, 1993.
35. L.B. Pankratz, "Thermodynamic Properties of Elements and Oxides," Bulletin 672, United States Department of the Interior, Bureau of Mines, 1982.
36. M. Yoshimura, "Phase Stability of Zirconia," Am. Ceram. Soc. Bull. 67 [12], pp. 1950–55 (1988).
37. O. Redlich, A.T. Kister, and C.E. Turnquist, "Thermodynamics of Solutions," Chem. Eng. Progress, Symp. Series, 48, pp. 49–64 (1952).
38. R.T. DeHoff, Thermodynamics in Materials Science, McGraw-Hill, 1993.
39. M. Hillert, Phase Equilibria, Phase Diagrams and Phase Transformation Their Thermodynamic Basis, Cambridge University Press, Cambridge, UK, 1998.
40. A.N. Belov and G.A. Semenov, "Thermodynamics of Binary Solid Solutions of Zirconium, Hafnium, and Yttrium Oxides from High-temperature Mass Spectrometry Data," Russ. J. Phys. Chem. 59 [3], pp. 342–44 (1985).
41. A.N. Belov, G.A. Semenov, G.A. Teterin, and T.M. Shkol'nikova, "Evaporation and Thermodynamic Properties of Sc_2O_3 and of ZrO_2-Sc_2O_3 Binary Solid Solutions According to High-temperature Mass Spectrometry Data II. Calculations," Russ. J. Phys. Chem. 61 [4], pp. 468–70 (1987),

TABLE I.—AVAILABLE BINARY PHASE DIAGRAMS

	ZrO_2	Y_2O_3	Yb_2O_3	Sc_2O_3	Nd_2O_3
ZrO_2		x	x	x	x
Y_2O_3			x	x	x
Yb_2O_3				x	x
Sc_2O_3					x
Nd_2O_3					

TABLE II.—ZIRCONIA AND RARE EARTH OXIDES TRANSITION TEMPERATURES AND HEATS OF TRANSFORMATION

Oxide	Phase Change	T(trans) K	$\Delta_{tr}H$ (kJ/mol)	$\Delta_{tr}S$ (J/mol-K)	Reference
ZrO_2	Monoclinic → Tetragonal	1448	5.941	4.103	Kubachewski (33)
	Monoclinic → Tetragonal	1478	8.075	5.464	Pankratz (35)
	Monoclinic → Tetragonal	1445	8.4	5.813	IVTAN (34)
	Tetragonal → Cubic	2568	5.9	2.3	Kubachewski (33)
	Tetragonal → Cubic	2620	13.001	4.962	IVTAN (34)
	Cubic → Liquid	2953	87	29.492	Kubachewski (33)
	Cubic → Liquid	2983	90	30.171	IVTAN (34)
Y_2O_3	Cubic → Hexagonal	2550	54	21.176	IVTAN (34)
	Hexagonal → Liquid	2712			Kubacheski (33)
	Hexagonal → Liquid	2712	81	29.867	IVTAN (34)
Yb_2O_3	Cubic → Hexagonal	2663			IVTAN (34)
	Hexagonal → Liquid	2708	130	48.006	IVTAN (34)
Nd_2O_3	N phase → Hexagonal				
	Hexagonal → Cubic	2333			IVTAN (34)
	Cubic → Liquid	2593	125	48.207	IVTAN (34)

TABLE III.—OXIDES AND ABBREVIATIONS

Oxide	Abbreviation
ZrO_2	ZM
$YO_{1.5}$	YM
$YbO_{1.5}$	BM
$NdO_{1.5}$	NM
$ScO_{1.5}$	SM

TABLE IV.—MOLE FRACTION OF RE_2O_3 IN RE_2O_3-ZRO_2 AND EQUIVALENT MOLE FRACTION OF $REO_{1.5}$ IN $REO_{1.5}$-ZRO_2

Mole Fraction RE_2O_3 $x(RE_2O_3)$	Equivalent Mole Fraction $REO_{1.5}$ $x(REO_{1.5})$
0.1	0.182
0.2	0.333
0.3	0.462
0.4	0.571
0.5	0.667
0.6	0.75
0.7	0.824
0.8	0.889
0.9	0.947

TABLE V.—EFFECT OF FIRST ORDER INTERACTION PARAMETER ON THE LOCATION OF THE MISCIBILITY GAP

Miscibility Gap	^1L
Symmetric	Zero
Shifted to Right	Positive
Shifted to Left	Negative

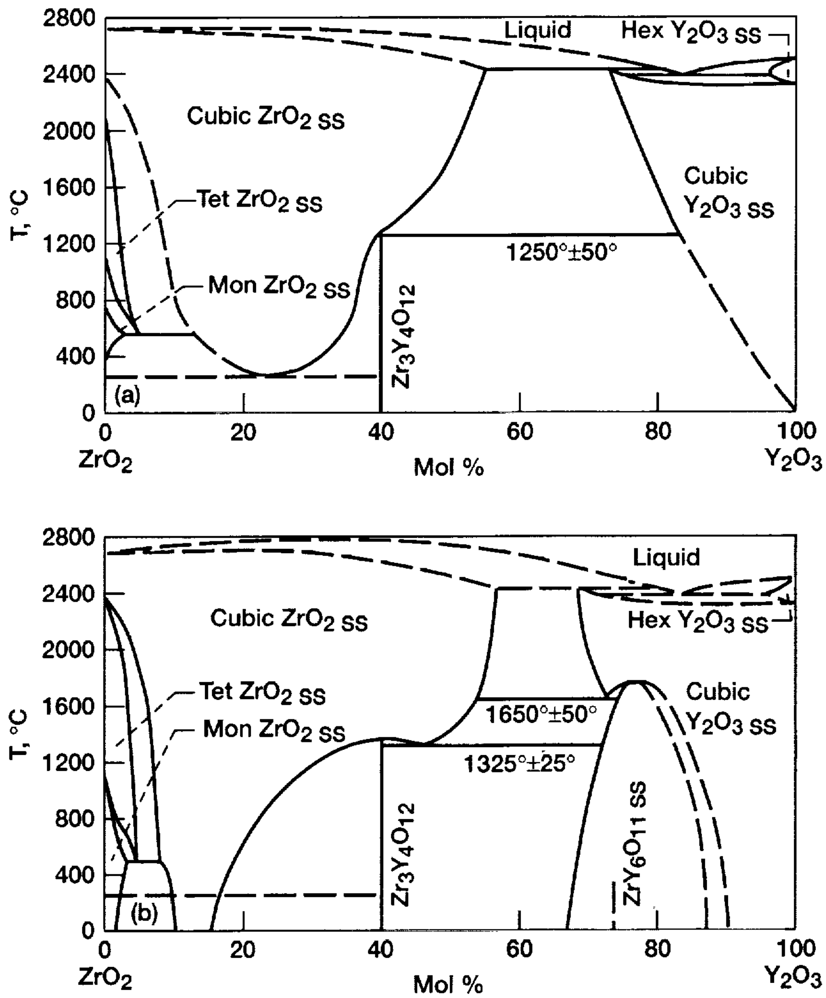

Figure 1.—Two experimentally determined Y_2O_3-ZrO_2 phase diagrams. (a) Stubican et al. 1981 (22, 7). (b) Pascual and Duran, 1983 (23, 9). Reprinted with permission of The American Ceramic Society, Post Office Box 6136, Westerville, OH 43086-6136. Copyright [1984] by the American Ceramic Society. All rights reserved.

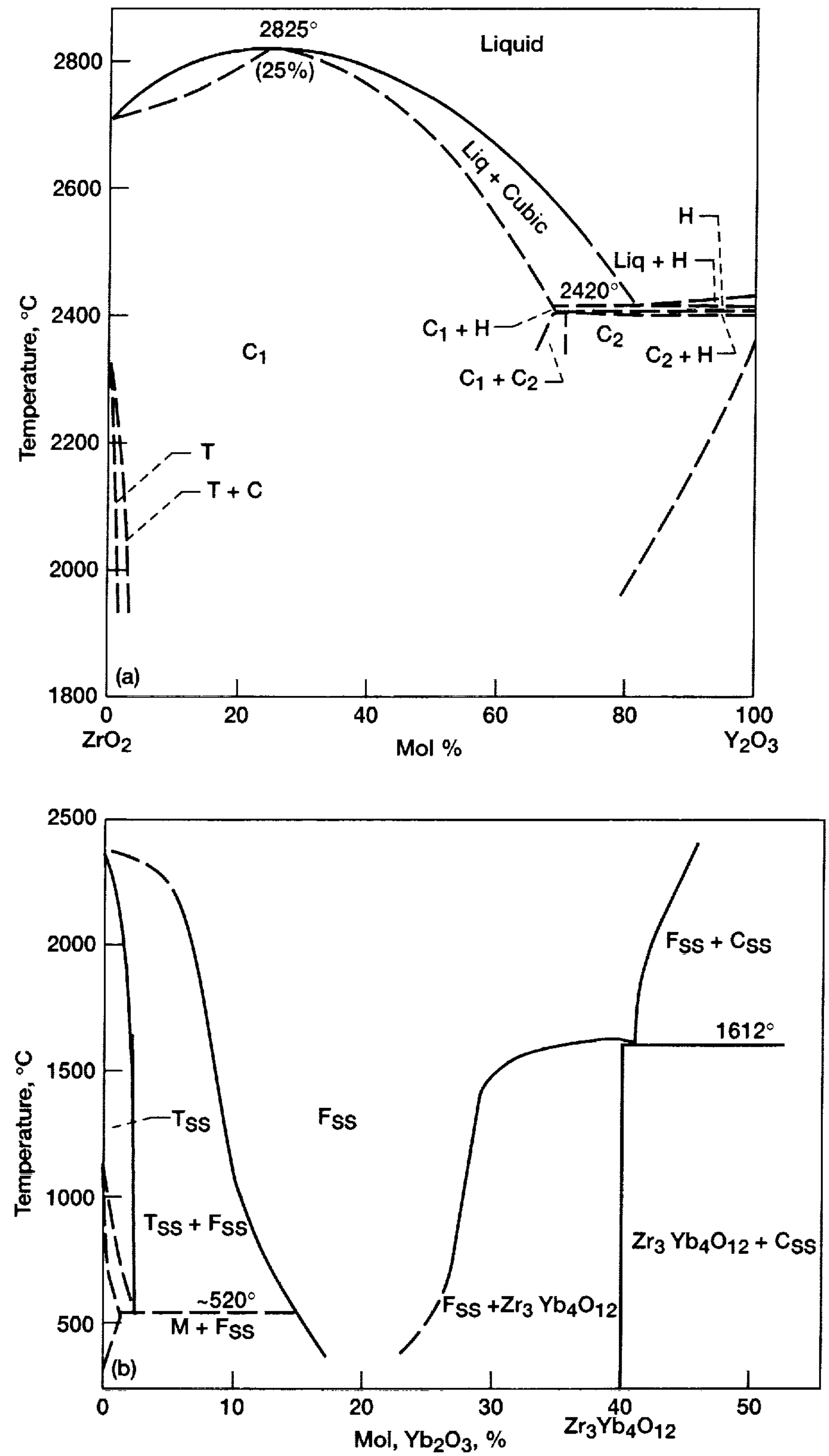

Figure 2.—Experimentally determined Yb_2O_3-ZrO_2 phase diagrams. (a) Rouanet (24). (b) Stubican et al. (11). Reprinted with permission of The American Ceramic Society, Post Office Box 6136, Westerville, OH 43086-6136. Copyright [1985] by the American Ceramic Society. All rights reserved.

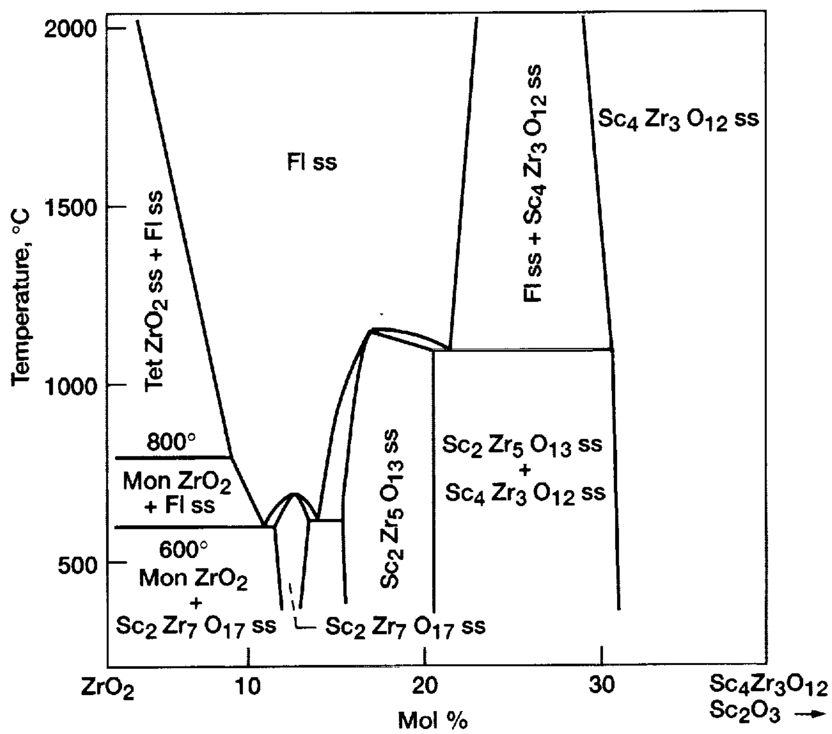

Figure 3.—Experimentally determined Sc_2O_3-ZrO_2 phase diagram (25). Reprinted with permission of The American Ceramic Society, Post Office Box 6136, Westerville, OH 43086-6136. Copyright [1993] by the American Ceramic Society. All rights reserved.

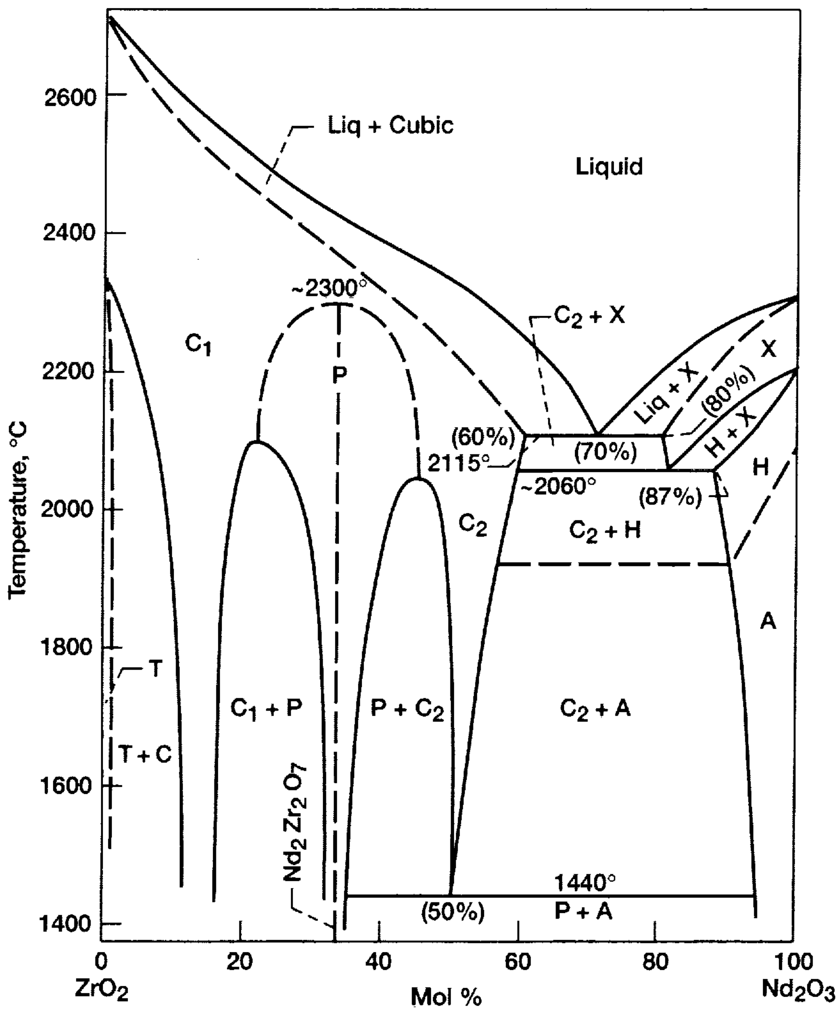

Figure 4.—Experimentally determined Nd_2O_3-ZrO_2 phase diagram (26). Reprinted with permission of The American Ceramic Society, Post Office Box 6136, Westerville, OH 43086-6136.

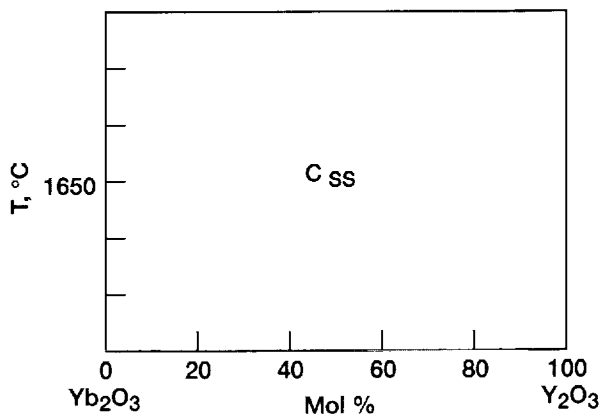

Figure 5.—Experimentally determined Yb_2O_3-Y_2O_3 phase diagram (27). Reprinted with permission of The American Ceramic Society, Post Office Box 6136, Westerville, OH 43086-6136. Copyright [1993] by the American Ceramic Society. All rights reserved.

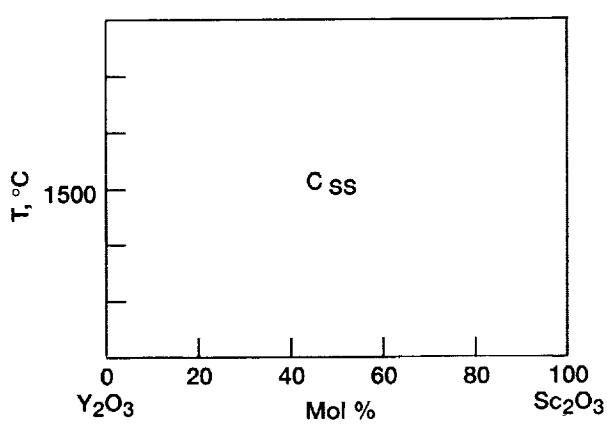

Figure 6.—Experimentally determined Sc_2O_3-Y_2O_3 phase diagram (28). Reprinted with permission of The American Ceramic Society, Post Office Box 6136, Westerville, OH 43086-6136. Copyright [1993] by the American Ceramic Society. All rights reservec

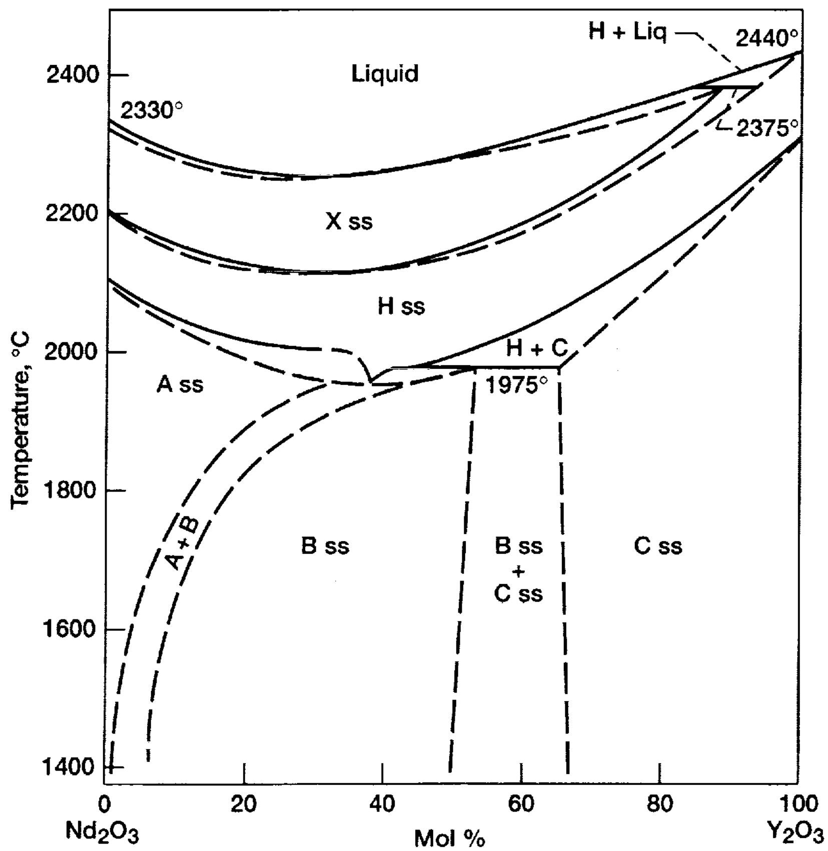

Figure 7.—Experimentally determined Nd_2O_3-Y_2O_3 phase diagram (29). Reprinted with permission of The American Ceramic Society, Post Office Box 6136, Westerville, OH 43086-6136. Copyright [1993] by the American Ceramic Society. All rights reserved.

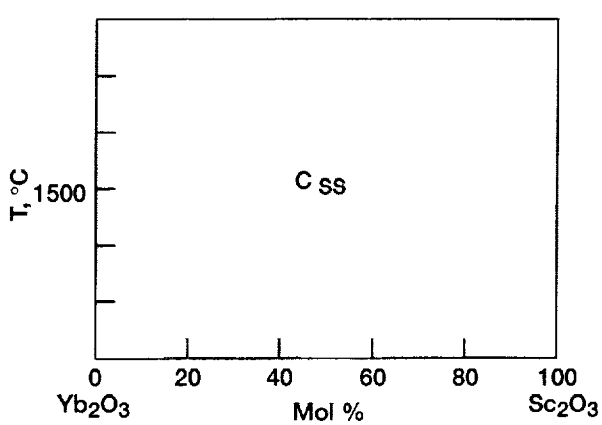

Figure 8.—Experimentally determined Sc_2O_3-Yb_2O_3 phase diagram (28). Reprinted with permission of The American Ceramic Society, Post Office Box 6136, Westerville, OH 43086-6136. Copyright [1993] by the American Ceramic Society. All rights reserved.

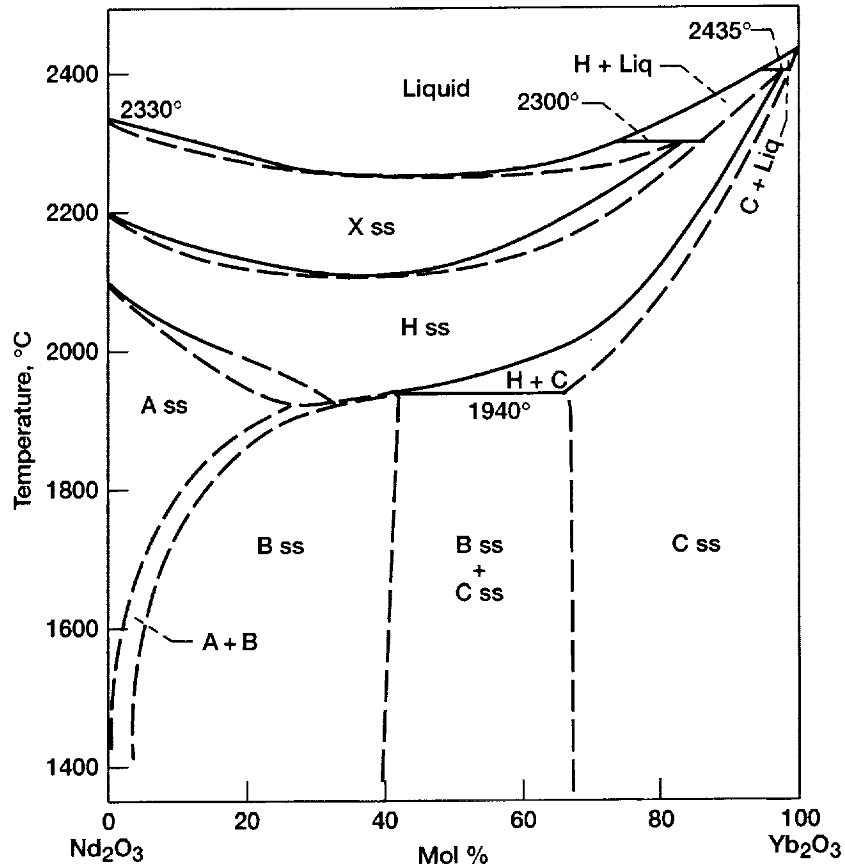

Figure 9.—Experimentally determined Nd_2O_3-Yb_2O_3 phase diagram (30). Reprinted with permission of The American Ceramic Society, Post Office Box 6136, Westerville, OH 43086-6136. Copyright [1993] by the American Ceramic Society. All rights reserved.

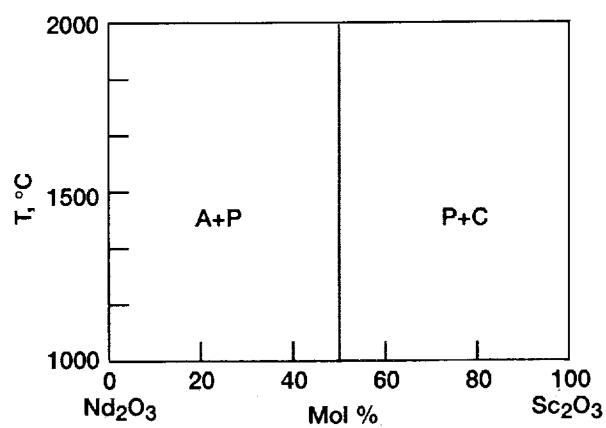

Figure 10.—Experimentally determined Nd_2O_3-Sc_2O_3 phase diagram (28). Reprinted with permission of The American Ceramic Society, Post Office Box 6136, Westerville, OH 43086-6136. Copyright [1993] by the American Ceramic Society. All rights reserved.

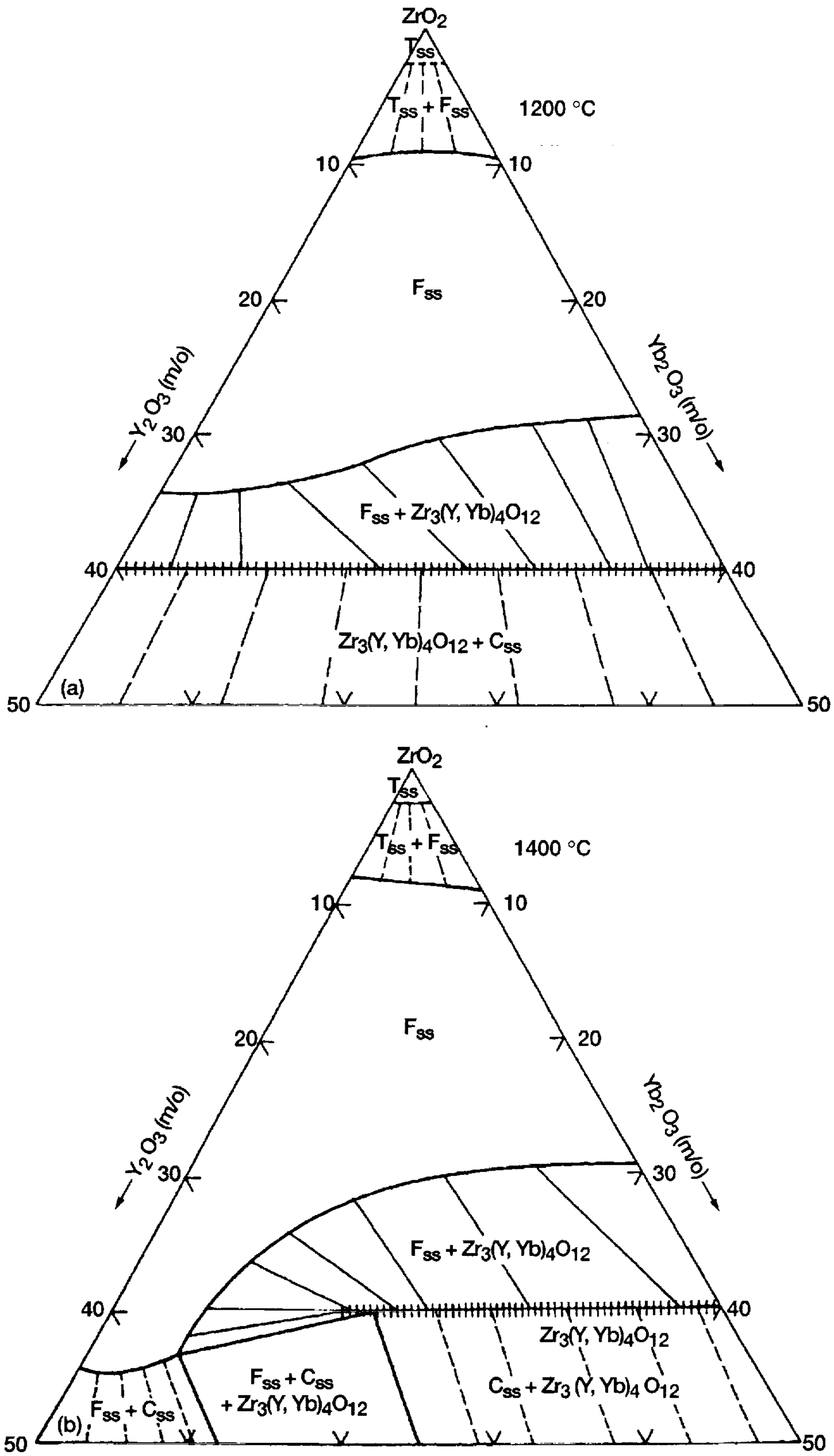

Figure 11.—Experimental determined Y_2O_3-Yb_2O_3-ZrO_2 phase diagram (31) at (a) 1200 °C, (b) 1400 °C, and (c) 1650 °C. Reprinted with permission of The American Ceramic Society, Post Office Box 6136, Westerville, OH 43086-6136. Copyright [1993] by the American Ceramic Society. All rights reserved.

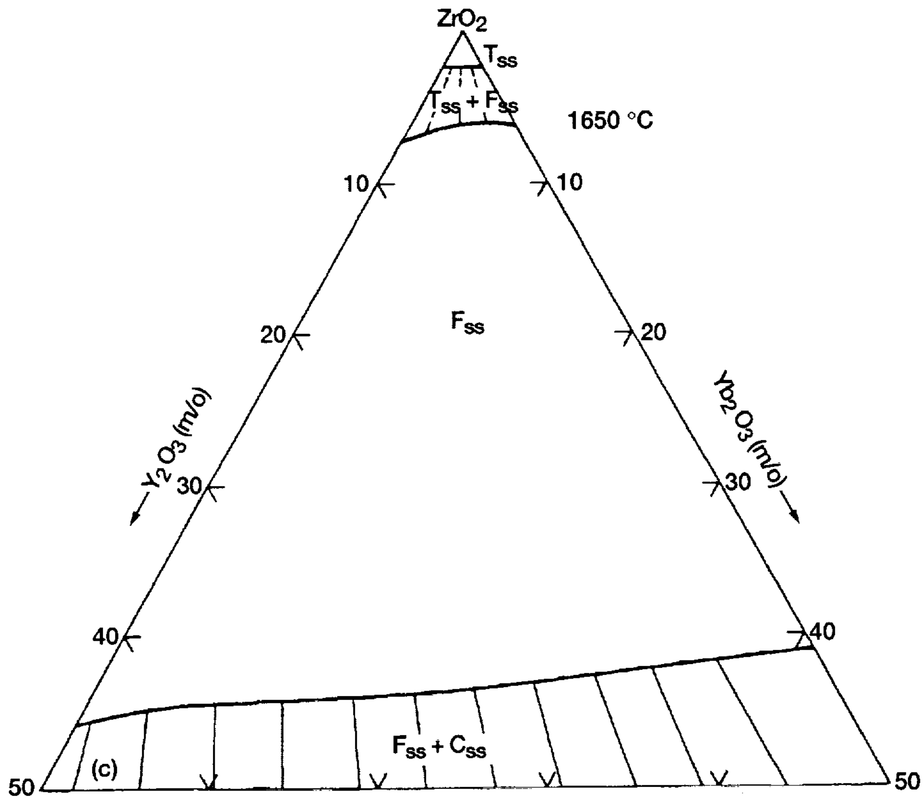

Figure 11.—Concluded. (c) 1650 °C. Reprinted with permission of The American Ceramic Society, Post Office Box 6136, Westerville, OH 43086-6136.

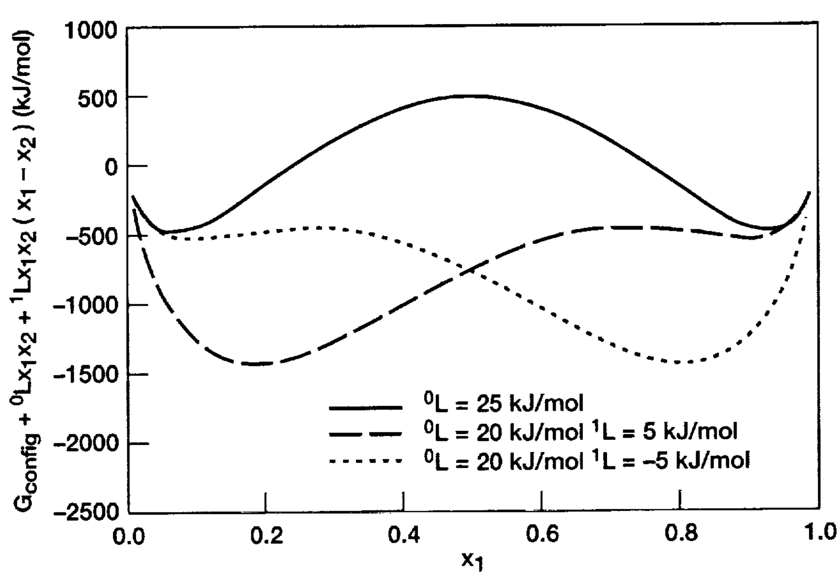

Figure 12.—Values of $G_{config} + G_{excess}$ versus T illustrating the effect of the interaction parameters on the symmetry and location of the miscibility gap.

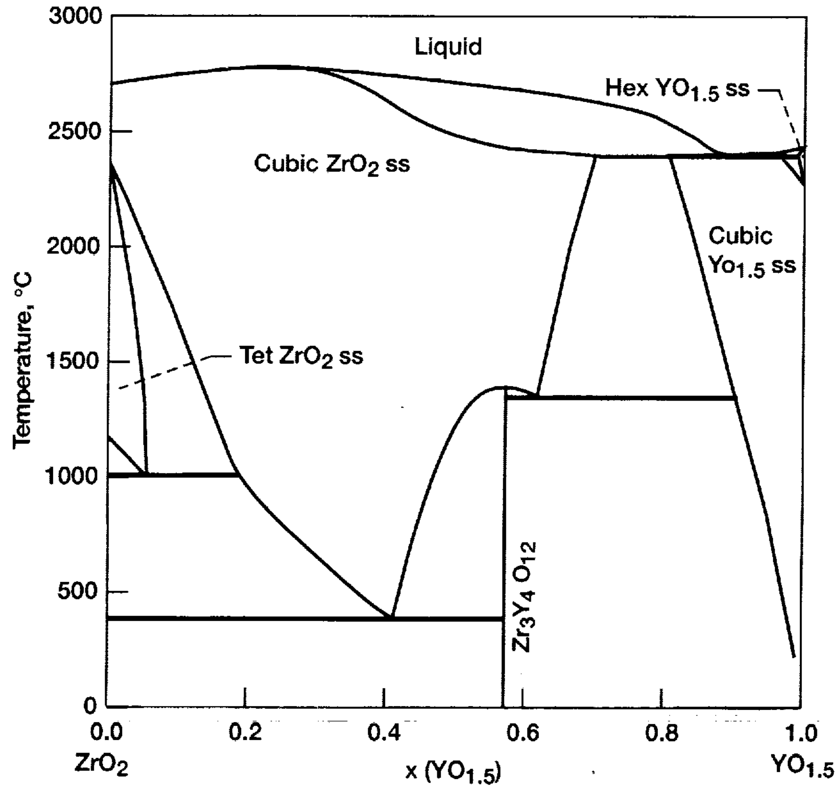

Figure 13.—Calculated $YO_{1.5}$-ZrO_2 phase diagram. Compare to Figure 1(a). The starting point for the calculation is x(YM) = 0.5, T = 3500 K.

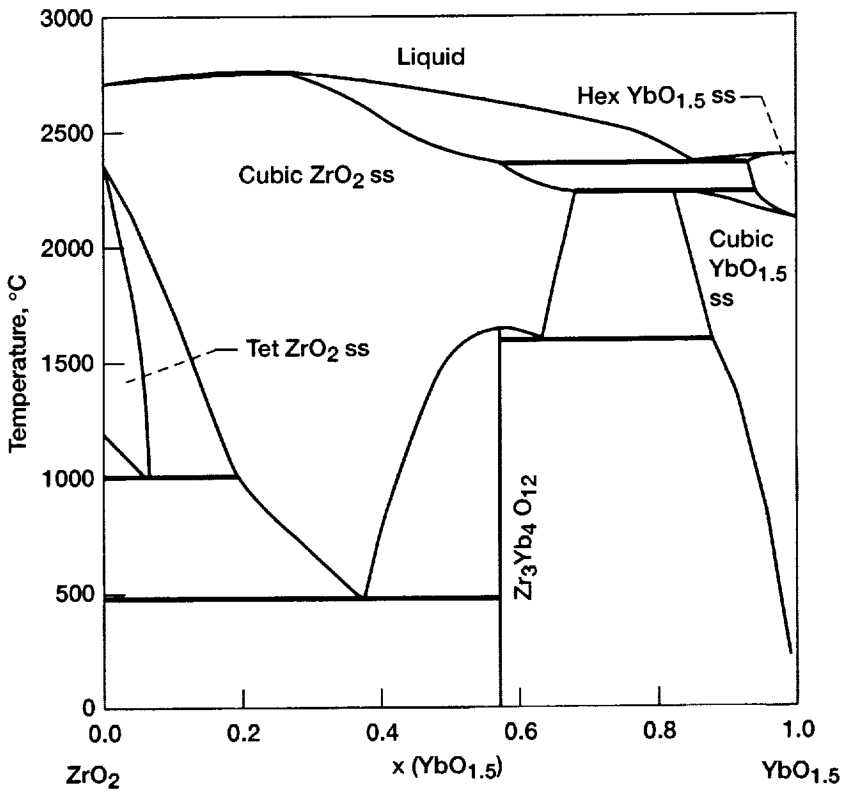

Figure 14.—Calculated $YbO_{1.5}$-ZrO_2 phase diagram. Compare to Figure 2. The starting point for the calculation is x(ZM) = 0.5, T = 3500 K, followed x(ZM) = 0.2, T = 2000 K.

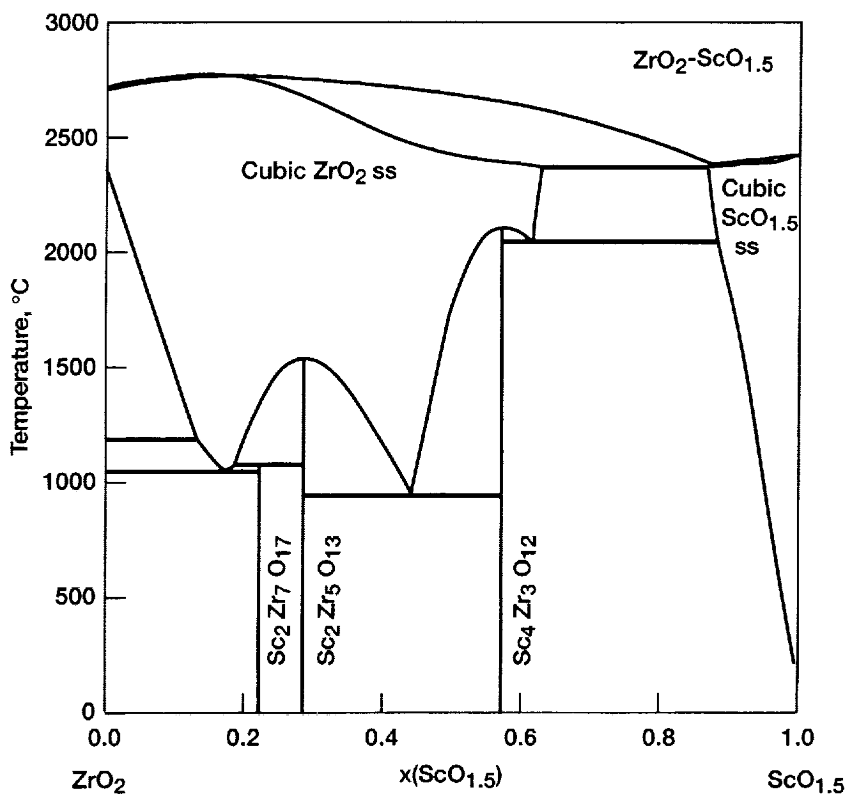

Figure 15.—Calculated $ScO_{1.5}$-ZrO_2 phase diagram. Compare to Figure 3. The starting point for the calculation is x(ZM) = 0.5, T = 3500 K.

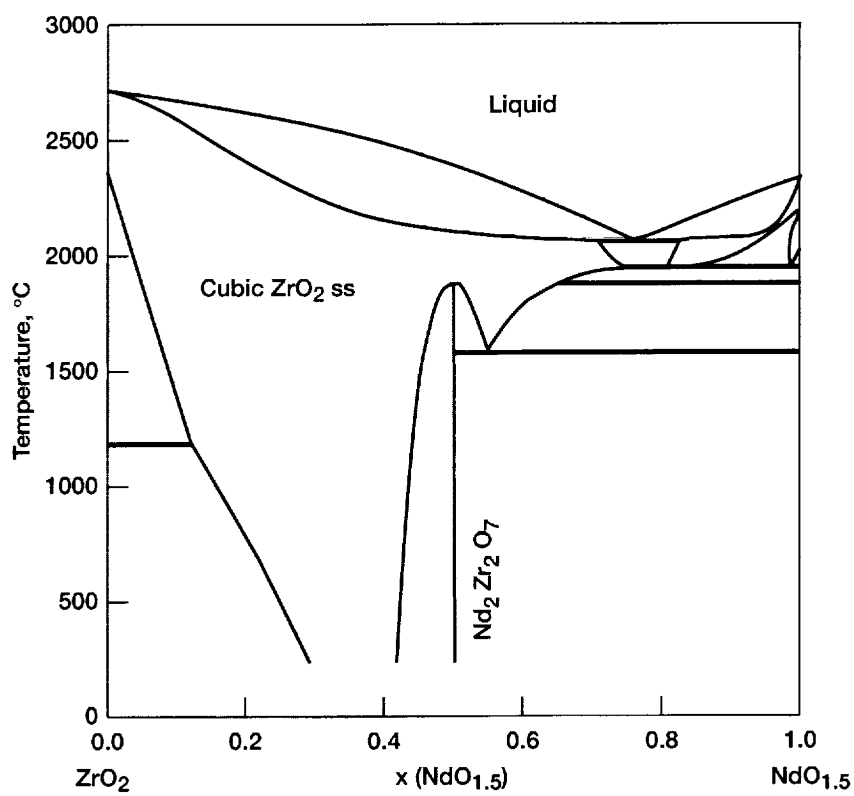

Figure 16.—Calculated $NdO_{1.5}$-ZrO_2 phase diagram. Compare to Figure 4. The starting point for the calculation is x(ZM) = 0.1, T = 1800 K, initially mapping up with temperature, followed by x(ZM) = 0.99, T = 1000 K, initially mapping up with temperature, followed by x(ZM) = 0.99, T = 3100 K, initially mapping up with temperature, and finally x(ZM) = 0.1, T = 2300 K.

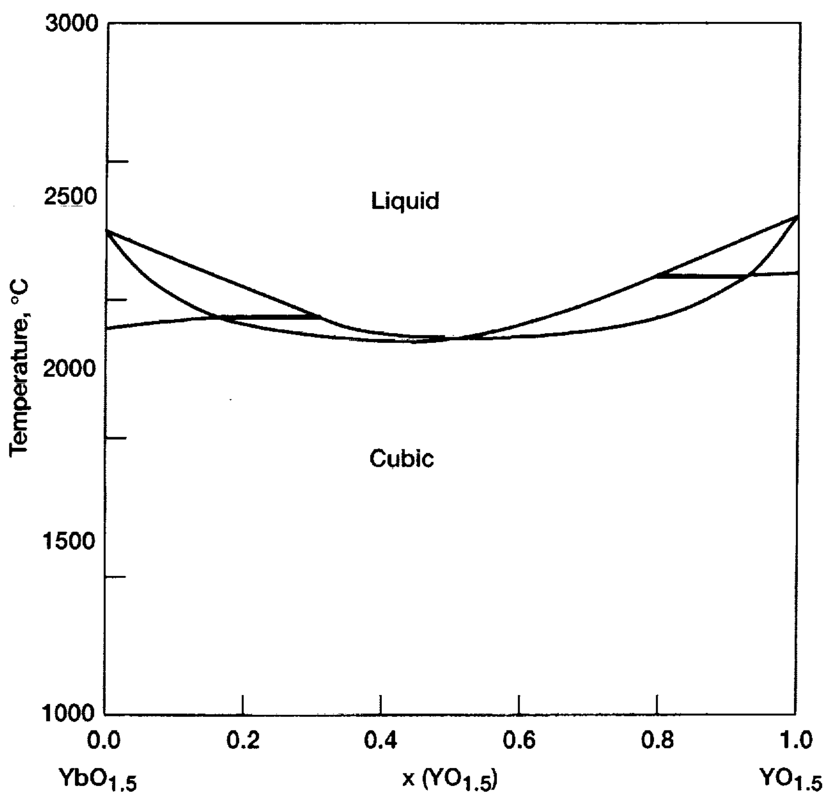

Figure 17.—Calculated $YbO_{1.5}$-$YO_{1.5}$ phase diagram. Compare to Figure 5. The starting point for this calculation is x(YM) = 0.001, T = 2500 K, map with temperature increasing first.

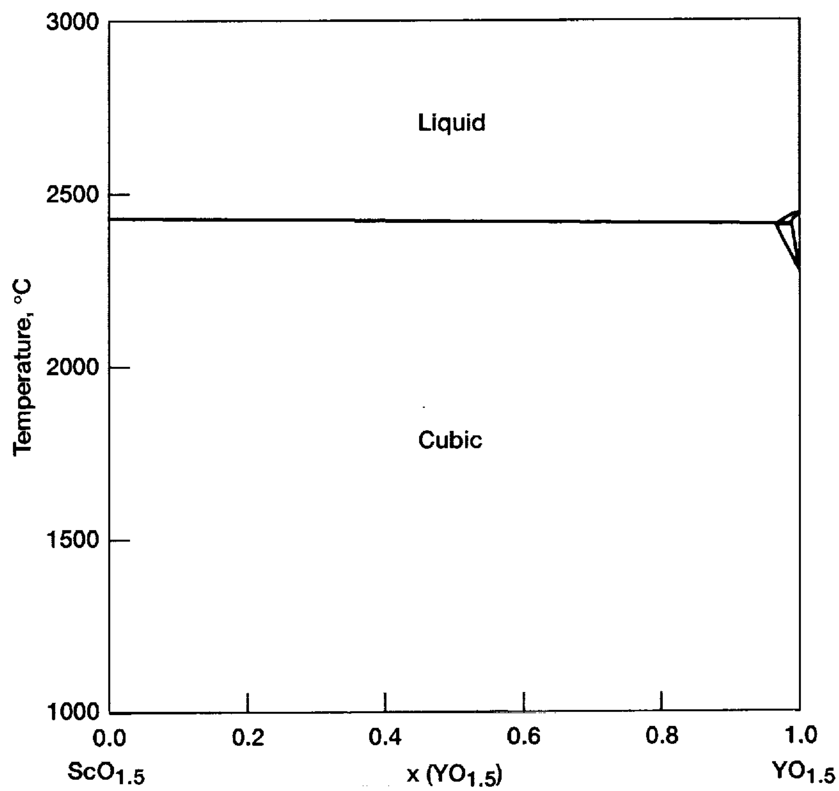

Figure 18.—Calculated $ScO_{1.5}$-$YO_{1.5}$ phase diagram. Compare to Figure 6. The starting point for this calculation is x(SM) = 0.001, T = 2500 K, map with temperature increasing first.

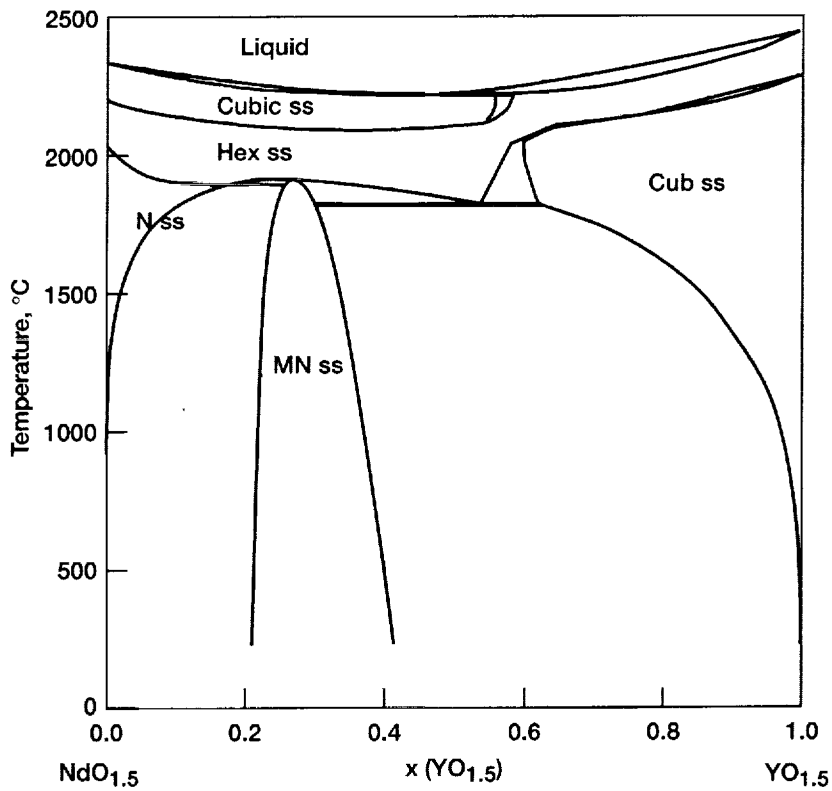

Figure 19.—Calculated $NdO_{1.5}$-$YO_{1.5}$ phase diagram. Compare to Figure 7. The starting point for this calculation is x(YM) = 0.01, T = 3000 K, followed by x(YM) = 0.99, T = 1500 K.

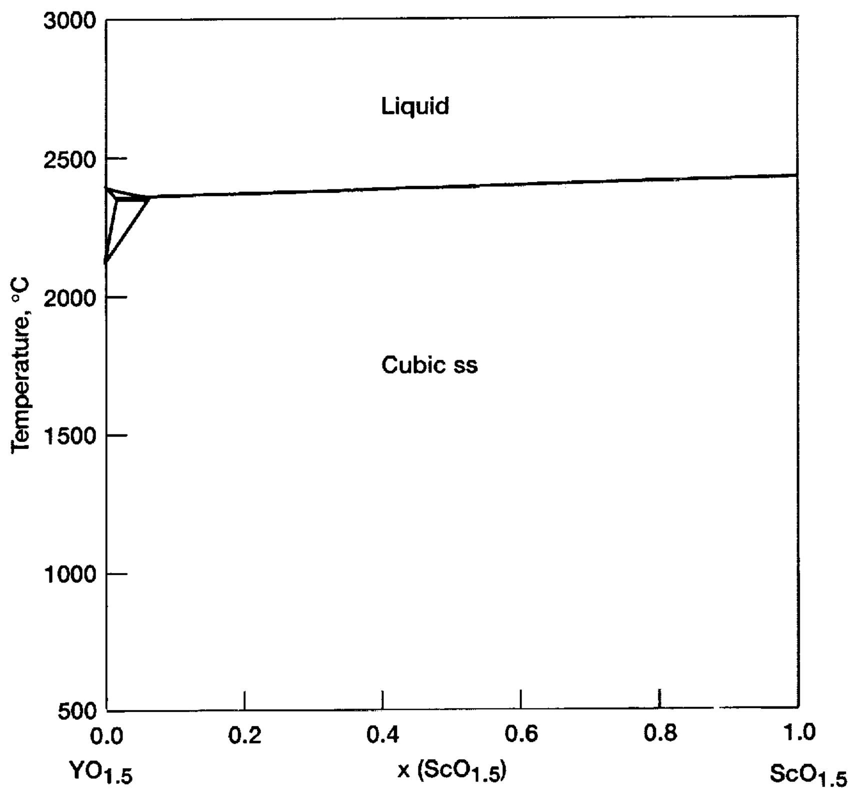

Figure 20.—Calculated $ScO_{1.5}$-$YO_{1.5}$ phase diagram. Compare to Figure 8. The starting point for this calculation is x(SM) = 0.001, T = 2500 K, map with temperature increasing first.

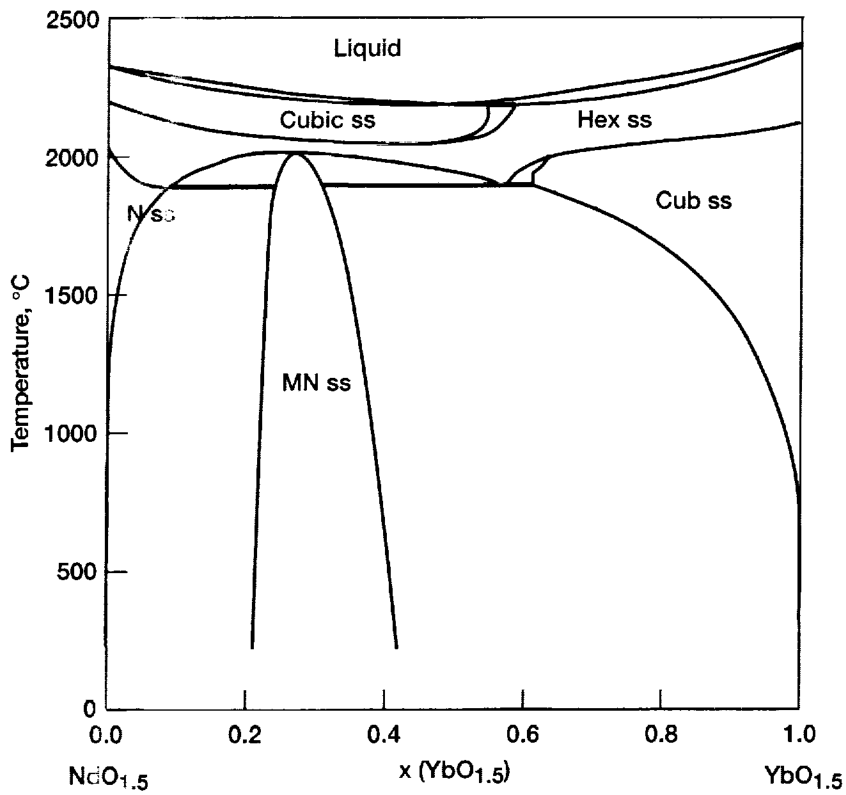

Figure 21 —Calculated $NdO_{1.5}$-$YbO_{1.5}$ phase diagram. Compare to Figure 9. The starting point for this calculation is x(BM) = 0.99, T = 3000 K, followed by x(BM) = 0.1, T = 1500 K.

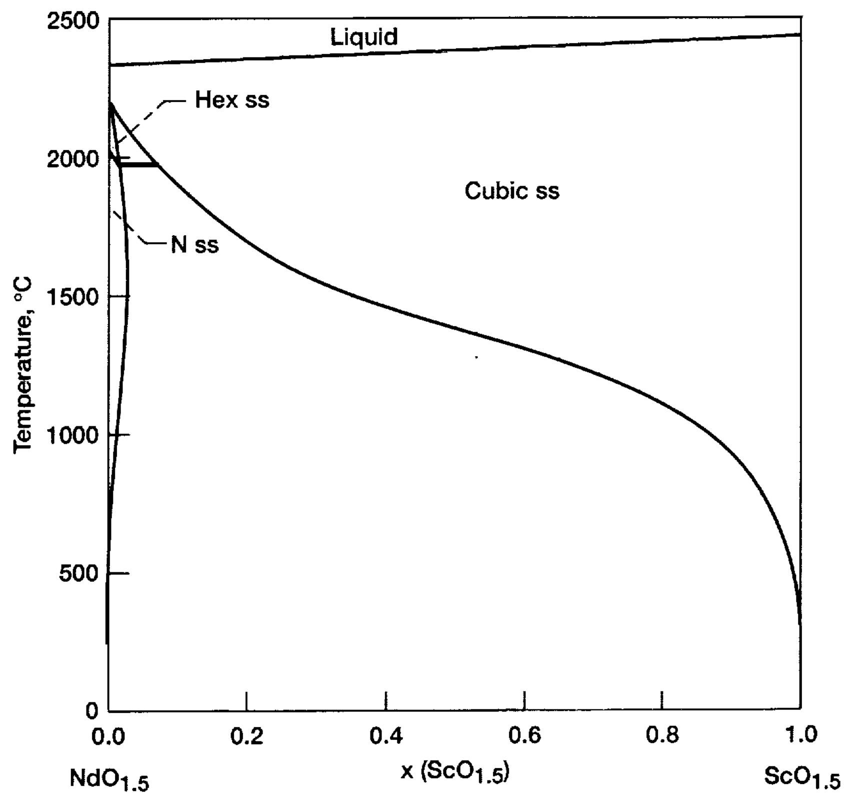

Figure 22.—Calculated $ScO_{1.5}$-$NdO_{1.5}$ phase diagram. Compare to Figure 10. The starting point for this calculation is x(SM) = 0.001, T = 3000 K, followed by x(SM) = 0.001, T = 1000 K.

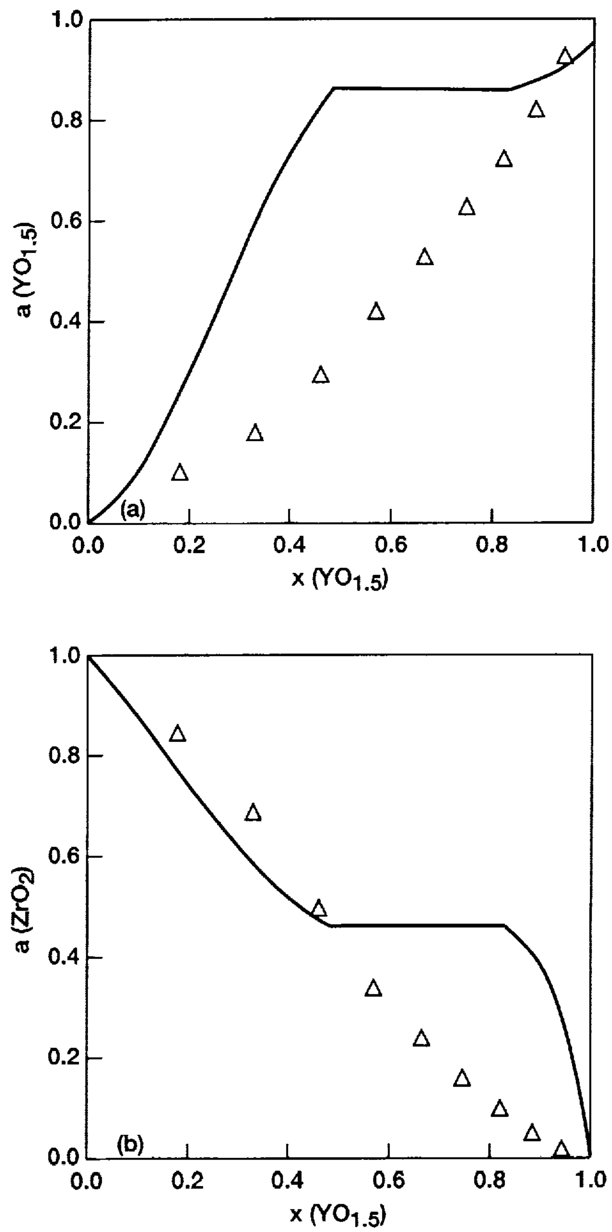

Figure 23.—Calculated activities across the $YO_{1.5}$-ZrO_2 phase diagram at 2773 K (line) and experimental data (points) of Belov and Semenov et al. (39). This line was generated using a starting point of x(ZM) = 0.8 and then a step with options command. (a) a ($YO_{1.5}$). (b) a (ZrO_2).

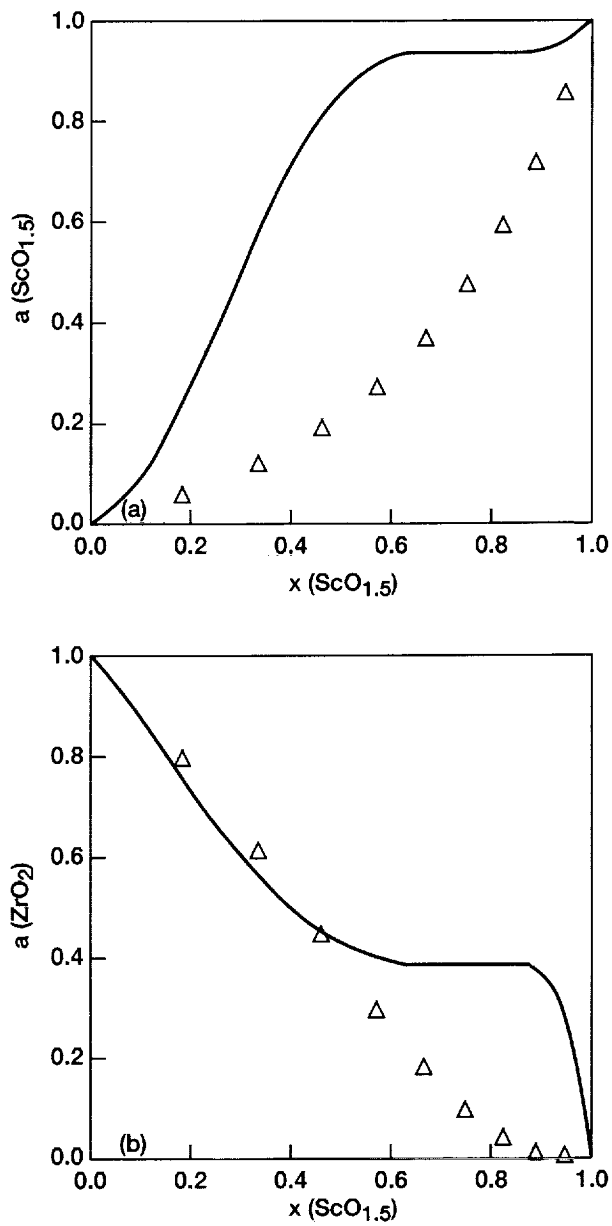

Figure 24.—Calculated activities across the $ScO_{1.5}$-ZrO_2 phase diagram at 2600 K (line) and experimental data (points) of Belov and Semenov et al. (40). This line was generated using a starting point of x(ZM) = 0.8 and then a step with options command. (a) a ($ScO_{1.5}$). (b) a (ZrO_2).

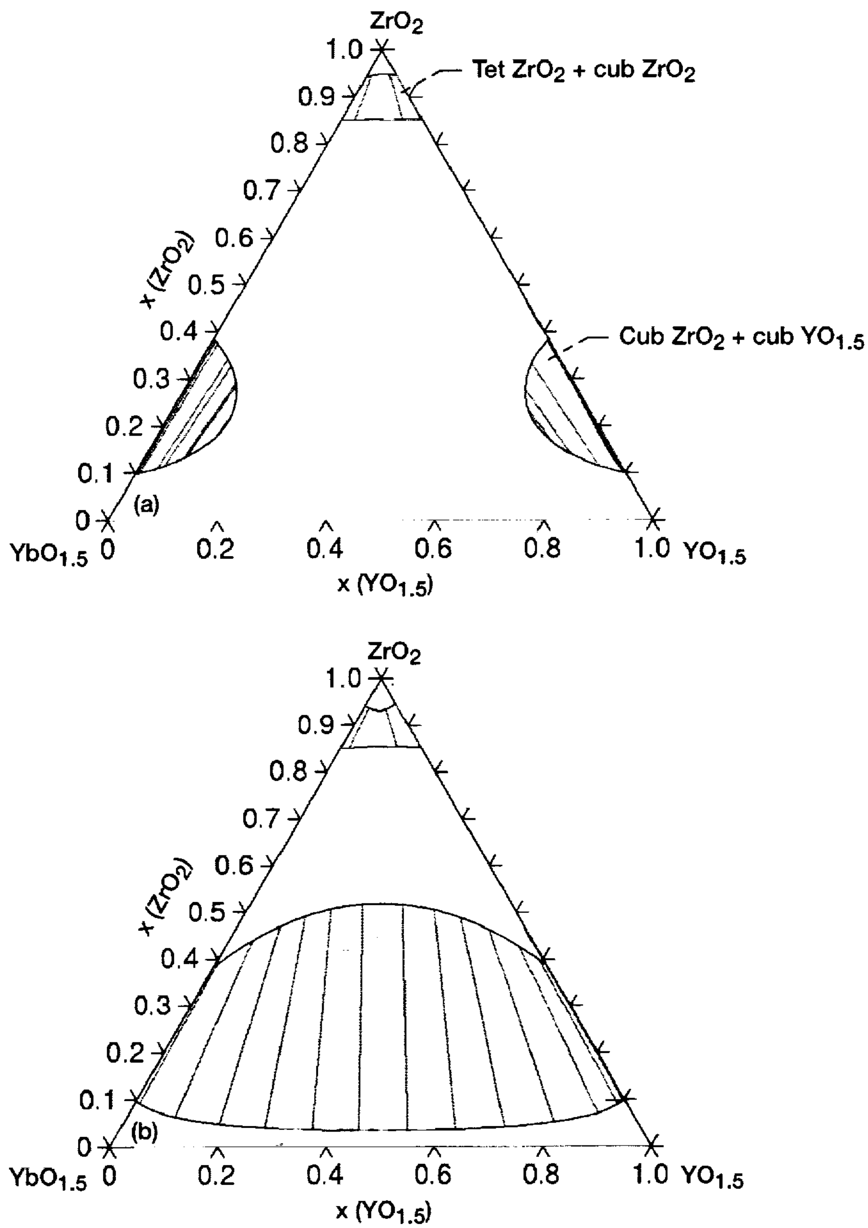

Figure 25.—Calculated ternary section for the $YbO_{1.5}$-$YO_{1.5}$-ZrO_2 system at 1600 K. (a) L(C, BM, YM, ZM; 0) = +10 000 insufficient to form a continuous two phase region. (b) L(C, BM, YM, ZM; 0) = +100 000 continuous two phase region.

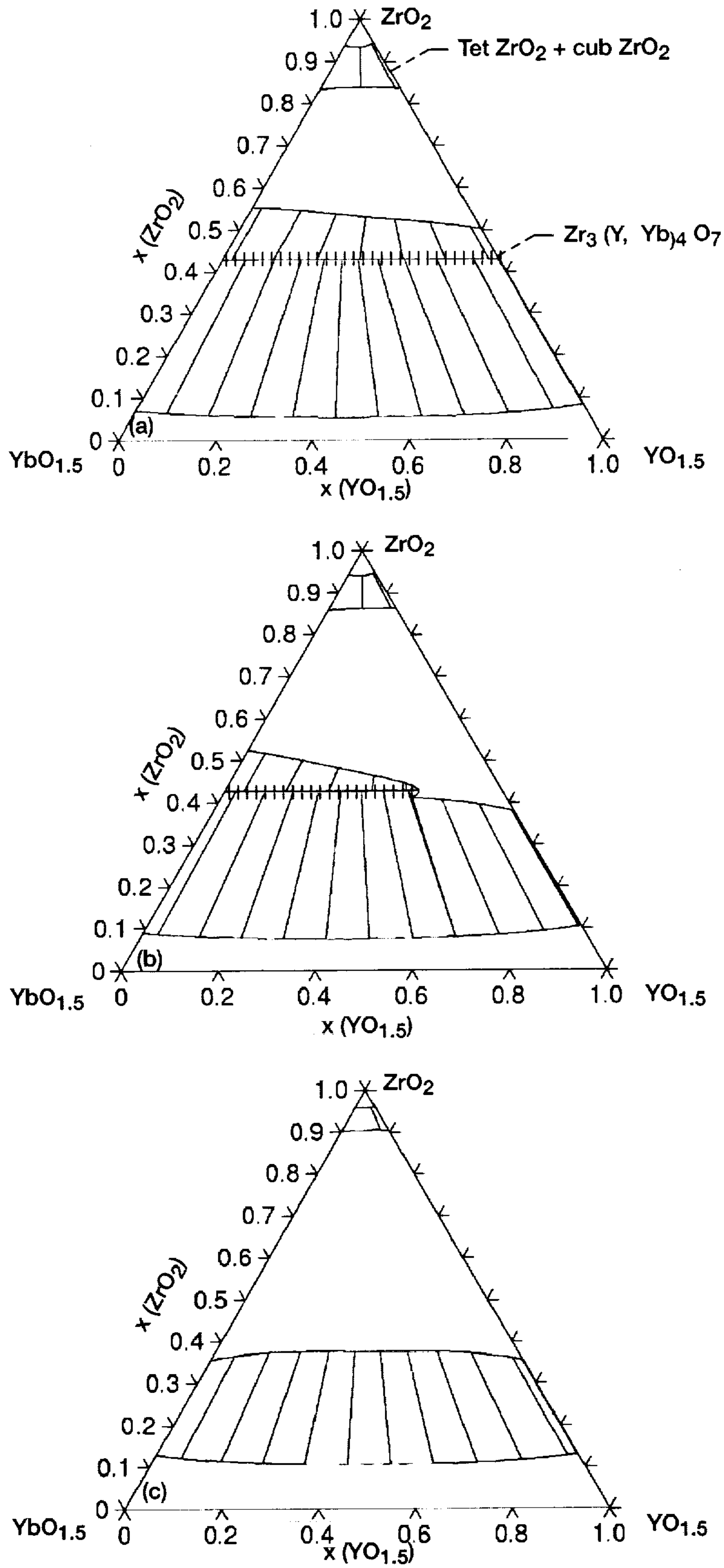

Figure 26.—Calculated ternary diagram for the $YbO_{1.5}$-$YO_{1.5}$-ZrO_2 system at (a) 1473 K, (b) 1673 K, and (c) 2000 K.

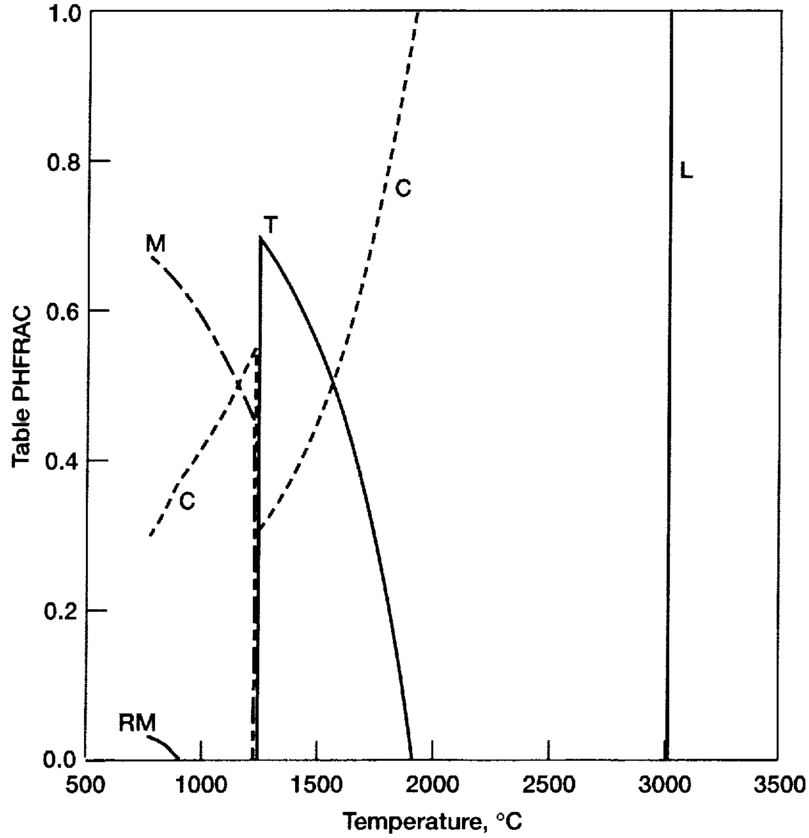

Figure 27.—Calculated phase fraction diagram for $0.05YbO_{1.5}$-$0.04YO_{1.5}$-$0.01ScO_{1.5}$-$0.9ZrO_2$.

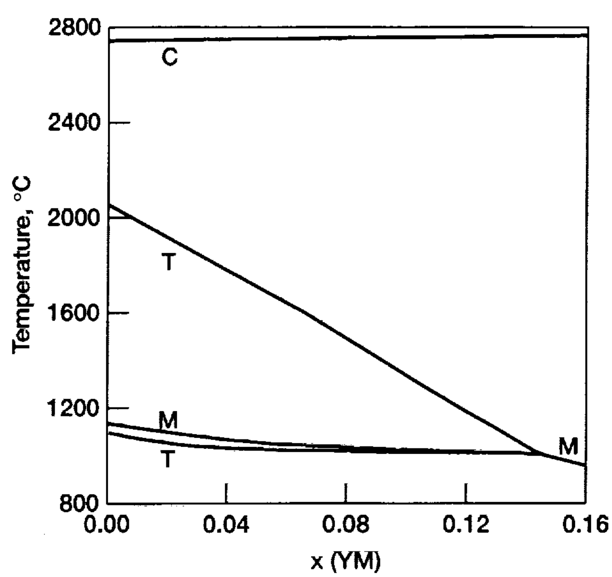

Figure 28.—Calculated isopleth for $YbO_{1.5}$-$YO_{1.5}$-$NdO_{1.5}$-ZrO_2 with $x(YbO_{1.5}) = x(ScO_{1.5}) = 0.02$.

REPORT DOCUMENTATION PAGE

Form Approved
OMB No. 0704-0188

1. AGENCY USE ONLY *(Leave blank)*

2. REPORT DATE
September 2001

3. REPORT TYPE AND DATES COVERED
Technical Memorandum

4. TITLE AND SUBTITLE
Thermodynamic Database for the $NdO_{1.5}$-$YO_{1.5}$-$YbO_{1.5}$-$ScO_{1.5}$-ZrO_2 System

5. FUNDING NUMBERS
WU-714-04-60-00

6. AUTHOR(S)
Nathan S. Jacobson, Evan H. Copland, and Larry Kaufman

7. PERFORMING ORGANIZATION NAME(S) AND ADDRESS(ES)
National Aeronautics and Space Administration
John H. Glenn Research Center at Lewis Field
Cleveland, Ohio 44135-3191

8. PERFORMING ORGANIZATION REPORT NUMBER
E-12681

9. SPONSORING/MONITORING AGENCY NAME(S) AND ADDRESS(ES)
National Aeronautics and Space Administration
Washington, DC 20546-0001

10. SPONSORING/MONITORING AGENCY REPORT NUMBER
NASA TM—2001-210753

11. SUPPLEMENTARY NOTES
Nathan S. Jacobson and Evan H. Copland, NASA Glenn Research Center; Larry Kaufman, Consultant, Brookline, Massachusetts 02445. Responsible person, Nathan Jacobson, organization code 5160, 216-433-5498.

12a. DISTRIBUTION/AVAILABILITY STATEMENT
Unclassified - Unlimited
Subject Categories: 25 and 27 Distribution: Nonstandard
Available electronically at http://gltrs.grc.nasa.gov/GLTRS
This publication is available from the NASA Center for AeroSpace Information, 301-621-0390.

12b. DISTRIBUTION CODE

13. ABSTRACT ***(Maximum 200 words)***

A database for $YO_{1.5}$-$NdO_{1.5}$-$YbO_{1.5}$-$ScO_{1.5}$-ZrO_2 for ThermoCalc (ThermoCalc AB, Stockholm, Sweden) has been developed. The basis of this work is the $YO_{1.5}$-ZrO_2 assessment by Y. Du, Z. Jin, and P. Huang, "Thermodynamic Assessment of the ZrO_2-$YO_{1.5}$ System," J. Am. Ceram. Soc. 74, [7], pp. 1569-77 (1991). Experimentally only the $YO_{1.5}$-ZrO_2 system has been well-studied. All other systems are only approximately known. The major simplification in this work is the treatment of each single cation unit as a component. The pure liquid oxides are taken as reference states and two term lattice stability descriptions are used for each of the components. The limited experimental phase diagrams are reproduced.

14. SUBJECT TERMS
Thermodynamics; Database; Ceramics

15. NUMBER OF PAGES
50

16. PRICE CODE

17. SECURITY CLASSIFICATION OF REPORT	18. SECURITY CLASSIFICATION OF THIS PAGE	19. SECURITY CLASSIFICATION OF ABSTRACT	20. LIMITATION OF ABSTRACT
Unclassified	Unclassified	Unclassified	